ANR-POSEIDON Deliverable D1.1: Scenario description KPIs and PHY requirements

Jean-Baptiste Doré, David Demmer, Rafik Zayani, Mabrouk Asma, Didier Le Ruyet, Hmaied Shaiek, Pascal Chevalier, Amor Nafkha, Haïfa Farès, Yoann Corre, et al.

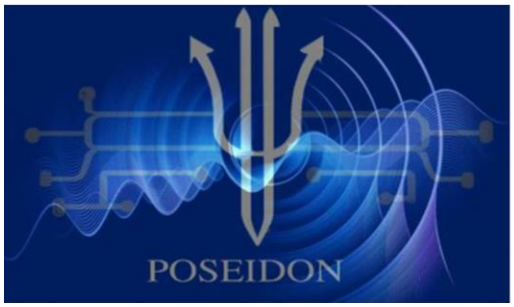

Funded by:
anr
Supported by:
ir
Images & Reseaux

Grant agreement ANR-22-CE25-0015

Deliverable D1.1

Scenario description KPIs and PHY requirements

Delivery date	20/09/2023
Version	1.0
Editor	Jean-Baptiste Doré – CEA Leti
Authors	Jean-Baptiste Doré, David Demmer, Rafik Zayani – CEA Leti Aymen Jaziri, Yoann Corre – SIRADEL Pascal Chevalier, Didier Le Ruyet, Hmaied Shaiek – CNAM Amor Nafkha, Haïfa Fares - CentraleSupelec
Dissemination	Public

History

Version	Date	Modification	Author(s)
1.0	20/09/2023	First version	See above

Executive summary

The POSEIDON project aims to define solutions for scalable CF-mMIMO operating in the sub-6GHz frequency bands (where the available spectral resources are scarce) toovercome various chanllenges (coverage, capacity, environmental sustainability…) . In particular, scalable CF-mMIMO architectures must be able to handle i) the dramatic increase in wireless traffic demand, which is caused by the exponential growth of connected wireless devices, and ii) the emerging services/applications requiring huge data traffic (e.g., high-quality video calls, holographic communications and Internet of Things/mMTC). Moreover, as an additional target, POSEIDON will propose architectures that may contribute in the roadmap for the necessary transition to greener solutions and infrastructures. With the ICT sector's power consumption increasing exponentially through the different generations of radio mobile networks, a tenfold increase of the power consumption for the wireless access is expected over the next decade. Thus, power consumption is among the critical key performance indicators (KPIs) to be optimized in 6G networks. To this end, POSEIDON will provide solutions to satisfy the expected 6G's requirements with ever-increasingly ubiquitous and reliable wireless connectivity while at the same time steadily addressing the crucial reduction of the ecological impact of cellular infrastructures. The project will focus on lower layers, physical and access, of CF-mMIMO where the consequences of these aforementioned objectives are direct and challenging.

This document presents a description of some applicative scenarios and use cases for CF-mMIMO systems which are envisaged in bands below 7GHz: dense mobile broadband network; multi service private network; Vehicular to Infrastructure network; and wide area MTC network. Two setups are proposed for the two first scenarios where studies can be realized on either a theoretical setup (properly configured to well capture the real environment characteristics) or a digital twin model (for better predictions accuracy).

An insight on the spectrum availability to deploy such wireless communications is provided. Key performance indicators are also given to evaluate and compare the different achieved technical performances and solutions. A preliminary list of KPIs per scenario with system parameters and performance requirements is also provided in this technical deliverable. A common PHY framework is given for performance assessments. It is worth mentioning that depicted KPIs values constitute a preliminary and an early shaping of targeted parameters for future CF-mMIMO wireless communications, which still need to be validated and confirmed.

Table of content

List of Acronyms

5G	5th Generation
5G-NR	5G New Radio
ADAS	Advanced Driver Assistance Systems
ADC	Analog to Digital converters
AI	Artificial Intelligence
AM/PM	phase deviation (PM) that is caused by amplitude variations (AM)
AP	Access Point
APM	Amplitude Phase Modulation
AWGN	Additive White Gaussian Noise
B5G	Beyond 5G
BBU	Baseband Unit
BEL	Building Entry Loss
BER	Bit Error Rate
BS	Base Station
CDL	Clustered Delay Line
CF-mMIMO	Cell Free massive MIMO
cmW	centimeter Wave
CN	Core Network
CP	Control Plan
CPE	Customer Premises Equipment
CPM	Continuous Phase Modulation
CPU	Central Processing Unit
C-RAN	Centralized RAN
CS-MUD	Compressive Sensing Multi User Detection
CU	Centralized Unit
D2D	Device to Device
DAC	Digital to Analog converters
DL	Downlink
DMRS	Demodulation reference signal
DPSK	Differential Phase Shift Keying
D-RAN	Distributed RAN
DU	Distributed Unit
EE	Energy Efficiency
EIRP	Equivalent Isotropic Radiated Power
eMBB	enhanced Mobile Broadband
FDD	Frequency Division Duplexing
FEC	Forward Error Correction
FSS	Fixed Satellite Systems
FWA	Fixed Wireless Access
GHG	GreenHouse Gases
GSM	Generalized Spatial Multiplexing
HWI	Hardware Impairment
ICS	Inter Carrier Spacing
ICT	Information and Communication Technologies

IM	Index Modulation
IoT	Internet of Things
IRR	Image Rejection Ratio
ITS	Intelligent Transport System
JT-CoMP	Joint transmission coordinated multi-point
KPI	Key Performance Indicator
KVI	Key Value Indicators
LiDAR	Light Detection and Ranging
LoS	Line-of-Sight
MAC	Medium Access Control
MEC	Mobile Edge Computing
MIMO	Multiple Inputs Multiple Outputs
mMIMO	Massive MIMO
mMTC	massive Machine Type Communications
mmWave	millimeter Wave
NB-IoT	Narroband IoT
NLoS	Non LoS
NOMA	Non-Orthogonal Multiple Access
O-CU	Open-Centralized Unit
O-DU	Open-Distributed Unit
OFDM	Orthogonal Frequency-Division Multiplexing
OOK	On Off Keying
O-RU	Open-Radio Unit
PA	Power Amplifier
PA	Power Amplifiers
PAPR	Peak to Average Power Ratio
PDCP	Packet Data Convergence Protocol
PER	Packet Error Rate
PHY-layer	Physical layer
PMR	Professional Mobile Radio
PN	Phase Noise
PN	Phase Noise
PSK	Phase Shift Keying
QAM	Quadrature Amplitude Modulation
QPSK	Quadratrure Phase Shift Keying
RAN	Radio Access Network
RE	Resource Element
RF	Radio Frequency
RLC	Radio Link Control
RRC	Radio Resource Control
RRH	Remote Radio Head
Rx	Receiver / Received
SCMA	Sparse Code Multiple Access
SE	Spectral Efficiency
SM	Spatial Multiplexing
SNR	Signal to Noise Ratio

SSPA	Solid State PA
TDD	Time Division Duplexing
TRL	Technology Readiness Level
TSN	Time-Sensitive Networking
Tx	Transmitter / Transmit
UE	User Equipment
UL	Uplink
ULA	Uniform Linear Array
UP	User Plan
URA	Uniform Rectangular Array
uRLLC	ultra Reliable Low-Latency Communications
V2I	Vehicle to Interface
V2X	Vehicle-to-Everything
VR	Virtual reality
V-RAN	Virtualized RAN
XR	encompasses augmented reality (AR), virtual reality (VR), and mixed reality (MR)

1 Introduction

1.1 Vision

The fifth generation (5G) wireless communications have been rolling out worldwide since 2019, providing high data rates, massive connectivity, ultra-reliability and low-latency. The key 5G technology is the massive multiple-input multiple-output (mMIMO), which is proposed by T. Marzetta in 2010 [1] . Massive MIMO, which deploys a large number of antennas at the base station (BS) in a co-located manner, can provide high spatial multiplexing gain, very low multi-user interference and low signal power variation. Thus, it offers high spectral efficiency (SE) and energy efficiency (EE). However, the fundamental limitation of co-located mMIMO is related to the inter-cell interference and large quality-of-service variations, making it incapable to cope with the challenges of the next/sixth generation (6G) wireless communications, demanding uniformly good user performance over the network coverage area [2]. Moreover, there are high demands for private networks and applications with rapid deployment of low-cost and energy-efficient wireless access infrastructures.

Towards this end, a revolutionary wireless network architecture is emerging, known as cell-free massive MIMO (CF-mMIMO), where no cell and cell boundaries exists. Note that CF-mMIMO technology exploits the best elements of i) network densification, ii) joint transmission coordinated multi-point (JT-CoMP) and iii) massive MIMO, while it avoids their drawbacks (a complete review is given in [3] Chapter 3, section 3.2.1). Two factors make CF-mMIMO different from the aforementioned technologies, which are the operating regime with a large number of access points (APs) compared to the number of served users together with the robust PHY layer advancements introduced for mMIMO; and the user-centric approach, i.e., each user (UE) is served by all the APs in its region of influence, stressing the cell-free aspect.

The fundamental idea of CF-mMIMO is to deploy a large number of distributed APs that are connected to a central processing unit (CPU). This latter is responsible to coordinate and process the signals of all served UEs. Consequently, the fronthaul capacity and the computational complexity are susceptible to grow exponentially with the number of users, affecting the network scalability [4]. To overcome this issue, a new version of CF-mMIMO was introduced in [4], namely scalable CF-mMIMO where fully distributed processing is adopted. In [5] and [6], authors introduced new scalable precoding and combining schemes together with channel estimation, power allocation methods, achieving very good benefits of CF-mMIMO. Therefore, the studies conducted within **POSEIDON** project will concern this scalable version of CF-mMIMO, aiming at developing signal processing-based solutions to satisfy the expected 6G's requirements with ever-increasingly ubiquitous and reliable wireless connectivity while at the same time steadily addressing the crucial reduction of the ecological impact of cellular infrastructures. The project will focus on lower layers, physical and access, of CF-mMIMO where the consequences of these aforementioned objectives are direct and challenging.

These solutions should be based on realistic propagation and hardware impairment (HWI) models, leading to practical solutions. Therefore, **POSEIDON** targets to identify and model relevant realistic propagation channels specific to CF-mMIMO systems, which are computationally challenging as compared to the classical/centralized massive MIMO systems. This process will allow the creation of

effective realistic and accurate channel models. Moreover, special attention will be given in order to also account for realistic hardware impairments (e.g. power amplifier non-linearities) leading to precise theoretical information analysis and accurate system transmission design related to the emerging CF-mMIMO technology.

Technological requirements. To assess the relevance of the proposed solutions with respect to the expectations, a study on the 6G Key Performance Indicators (KPIs) and Key Value Indicators (KVIs) will be conducted.

Air interface enablers for CF-mMIMO. The basic signal processing concepts for communication, backhauling, and access will be made practical by addressing realistic limitations such as heterogeneous infrastructure, computational capabilities and scalability. Specifically, we will develop and enhance algorithms for channel estimation, data transmission/reception, PHY security, initial access signalling, proper trade-offs for different 6G use-cases, KVIs, and KPIs.

Radio resource management enablers for CF-mMIMO. The dense AP deployment requires reliable but lean cooperation to make practical use of the available radio resources. Specifically, we will develop theory and algorithms that enable efficient, robust, and scalable mobility management, scheduling, pilot and power allocation, dynamic AP clustering, and allocation of computational tasks

1.2 Path toward 6G

During the last decades, the world of wireless communications has evolved from the Voice Era (1G) to the Mobile Broadband Era (3G) and has now entered the Super Connected Era, enabled by the enhanced Mobile Broadband (eMBB), massive Machine Type Communications (mMTC) and ultra Reliable Low-Latency Communications (uRLLC) use-cases of 5G. 6G will further improve the technical performance of these use cases but is expected to make radical developments beyond the purely technical requirements, leveraging a human-centric societal approach that targets inclusivity, natively integrated Artificial Intelligence (AI), end-user engagement, trustworthy technology, and sustainability.

According to [7], Mobile network data traffic grew 38% between Q3 2021 and Q3 2022 and has almost double in the last two years. This increase is driven by both the rising number of smartphone subscriptions and an increasing average data volume per subscription, fuelled primarily by videos content (download and upload). Video services alone account for about 70% of traffic in 2022 as depicted in Figure 1.

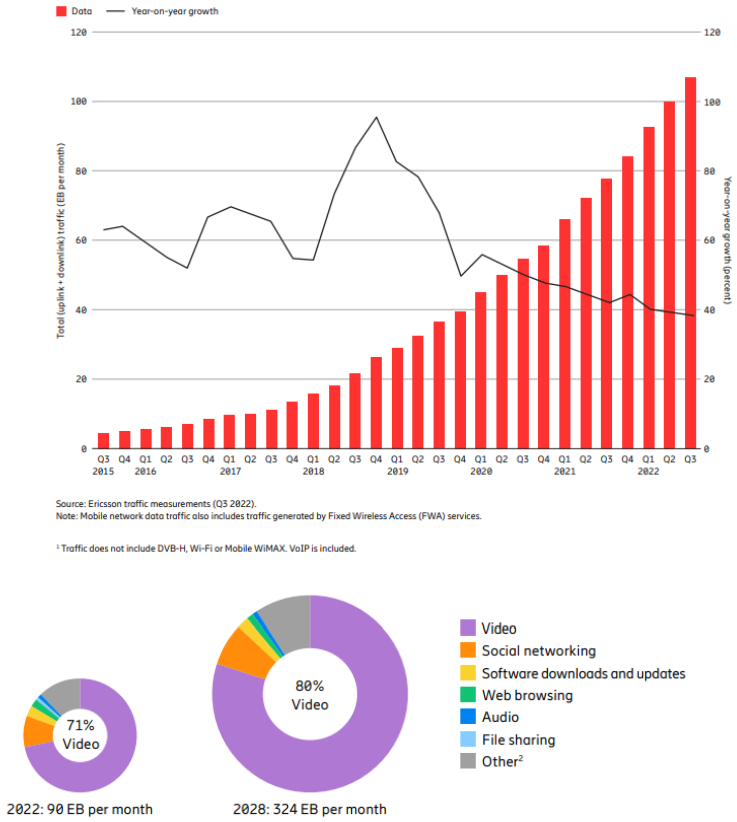

Figure 1 – Global mobile network data traffic and year-on-year growth (EB per month) and Mobile data traffic by application category per month from [7].

Despite dramatic efficiency and productivity improvements, the Information and Communication Technologies (ICT) GreenHouse Gases (GHG) emissions have dramatically risen. The current trajectory of the digital and telecommunication sectors is thus not compatible with earth limits as the world's carbon emissions must shrink. The ICT sector is estimated to consume 6.4% of the world-wide electricity and generates between 2.1% and 3.9% of the world-wide CO_2 emissions. This percentage equals the global civil air traffic contribution and 1⁄4 of the CO2 emissions by all vehicles. It is expected that ICT will produce up to 7.4% of the global emissions by 2030 and 14% by 2040, unless radically new solutions are developed to change the trajectory.

For 6G to fulfill performance, societal and environmental expectations, a paradigm shift is needed, requiring the design of new networks and the exploration of new spectrum bands. In this context, the CF-mMIMO technology is a candidate technology that help reaching the 6G requirements. This technology will be studied in our project.

The use of centimeter Wave (cmW) spectrum is a key choice for 6G as it complements the 3.5 GHz band and millimeter Wave (mmW) band utilized by 5G. With an acceptable link budget even for outdoor-to-indoor links and the possibility to deploy digital panels with large antenna numbers in small enclosures, these bands are particularly well suited for network densification and mMIMO spatial multiplexing and beamforming.

POSEIDON has the ambition to demonstrate that CF-mMIMO is a 6G enabler, compatible with the new societal and environmental expectations. 6G in general, and CF-mMIMO in the cmW in particular, are fresh research topics that currently have a low Technology Readiness Level (TRL). Several issues and challenges must be tackled before this technology can be rolled out in practice. To address these issues, POSEIDON will focus on a set of identified key research areas.

1.3 Spectrum candidates

Several applications drive the rise in frequency of wireless networks ranging from the ever-increasing mobile traffic to the recent emergence of new applications like Industry 4.0. The mid-band, i.e. the 3.0-6.0 GHz spectrum, proves to be relevant as it provides large bandwidths and good propagation properties. Besides, hardware operating at those frequencies are available at shorter notice than mmWave. This spectrum is thus relevant for applications already deployed below 3.0 GHz like mobile broadband (eMBB) and Internet of Things (IoT) as shown in Figure 2. Applications with tougher data rate and latency requirements are expected to be mainly deployed at 26.0 GHz and above; however a deployment in the mid-bands is generally considered as well.

Use case	Low bands	Mid-bands	mmWave bands
eMBB	10%	80%	10%
FWA	10%	60%	30%
MIoT	40%	60%	0%
URLLC	0%	40%	60%

Figure 2 - Use cases and relevance spectrum band [8].

There is therefore a need to investigate the use of the mid-band spectrum in parallel to the mmWave spectrum and above. In the following sections, the specific visions for the 3.8-4.2 GHz and 6.0-7.0 GHz bands will be detailed.

1.3.1 Mid-frequency spectrum

The mid-frequency spectrum (roughly from 3.3 GHz to 4.2 GHz) offers an interesting trade-off between coverage and capacity and can therefore meet the demand for mobile broadband traffic. Mid-band spectrum has globally been considered for 5G high-capacity city-wide coverage. In addition to that, their use cases will keep growing with the deployment of Fixed Wireless Access (FWA) and the emergence of wireless industrial networks (e.g. Industry 4.0) [8]. Indeed, the European Commission has identified the demand for sub-6GHz licensed bands for non-cellular applications and is investigating the shared and harmonized use of the 3.8-4.2 GHz frequency band [9]. In parallel,

international markets and countries are opening spectrum for companies to build their own private network. Here are some recent examples for the mid-band frequencies:

	November 2019	BNetzA allocates 100 MHz at 3.7 GHz set aside for industrial, agricultural and other private networks. 215 licences have been granted (November 2022).
	March 2022	Arcep provides licences for up to 100 MHz at 3.8-4.0 GHz (experiments, 3-year deal). 25 licences have been delivered (February 2023)
	January 2023	Nikom opens licences for 20,40,60 and 80 MHz at 3.8-4.2 GHz dedicated to standalone private network (10-year deal)
	January 2023	PTS invites applications for spectrum at 3.7 GHz (80 MHz bandwidth).

Harmonizing the use of spectrum between countries is challenging because regulators' approach widely differ. For instance in Europe, some countries have dedicated licensed spectrum for industrial applications (e.g. Germany and France) while others have forced 5G network providers to lease part of their cellular bands to industries (e.g. Czech Republic and Denmark).

1.3.2 Upper-6GHz Spectrum

Lately, the 6 GHz band also gained in attractiveness with for instance the rise in frequency of Wi-Fi networks with a focus on the 5.925-7.125 GHz [9] and cellular networks with a focus on the 6.425-7.125 GHz for release 17 and 5.925-7.125 MHz for release 18 [11]. There is a real need for additional spectrum to support the ever-increasing data traffic, as depicted in Figure 3.

The motivations to consider the 6 GHz spectrum are multiple:

- It is possible to reuse the same infrastructure of the 3.5 GHz network which enables a cost-effective deployment [11].
- The infrastructures and products are available at short notice [11].
- The hybrid licensed-unlicensed approach is considered for the band to facilitate the spectrum sharing with other networks: unlicensed for the 5.925-6.425 MHz and licensed for the 6.425-7.125 MHz.

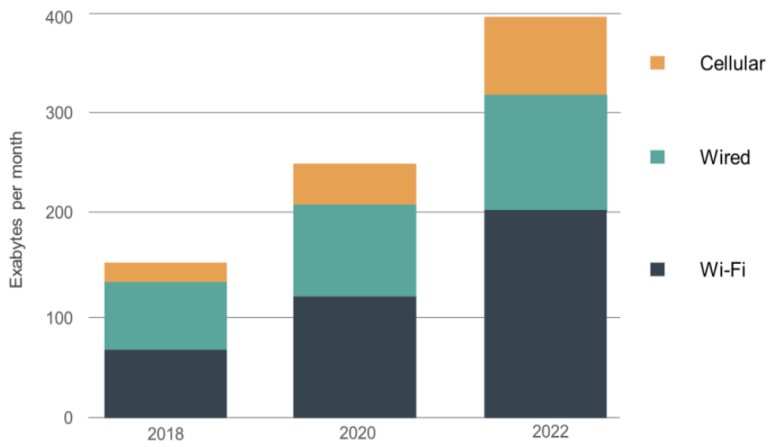

Figure 3 – Data traffic increase (from [11])

If one focuses on Wi-Fi networks, Wi-Fi 7 will support 3 320-MHz channels in the 6 GHz spectrum (7 160-MHz for Wi-Fi 6E). Besides, although Wi-Fi was long dedicated to end user connectivity, its use cases have now diversified ranging from IoT, smart house applications and healthcare. Wi-Fi eases the deployment of new applications as it inherently integrates security and authentication processes. Besides, Wi-Fi can efficiently share the spectrum with other incumbents (such as cellular links and Fixed Satellite Systems (FSS) for the 6 GHz spectrum) thanks to its power management. That is why Wi-Fi is likely to become a solid solution for non-critical business traffic.

The increased building penetration loss is a major inconvenience for a network technology that aims at providing global coverage at higher frequency. In particular, this is known to be a critical limitation for indoor coverage by an outdoor network operating in the millimetre-wave spectrum or above. The ITU-R P.2109 recommendations [12] permit to estimate what would be the impact of building penetration at frequencies 6 or 7 GHz. Those recommendations propose a statistical model for the building entry loss (BEL), based on the analysis of a rich measurement dataset collected in the range from 80 MHz to 73 GHz. Note that the considered BEL includes both “the loss suffered by a signal penetrating the exterior wall and the attenuation suffered in the path through the building”. The median BEL value at horizontal incidence is shown in Figure 4 for various frequencies and two different kinds of building i.e., traditional or energy-efficient. We added the values calculated at frequencies 3.5 GHz (our 5G network reference) and 7 GHz (the frequency of interest in the project). It appears that the median building loss increases by 1.2 dB and 1.7 dB for respectively the traditional and energy-efficient buildings, which is an additional constraint for global indoor coverage, but is not an insurmountable obstacle.

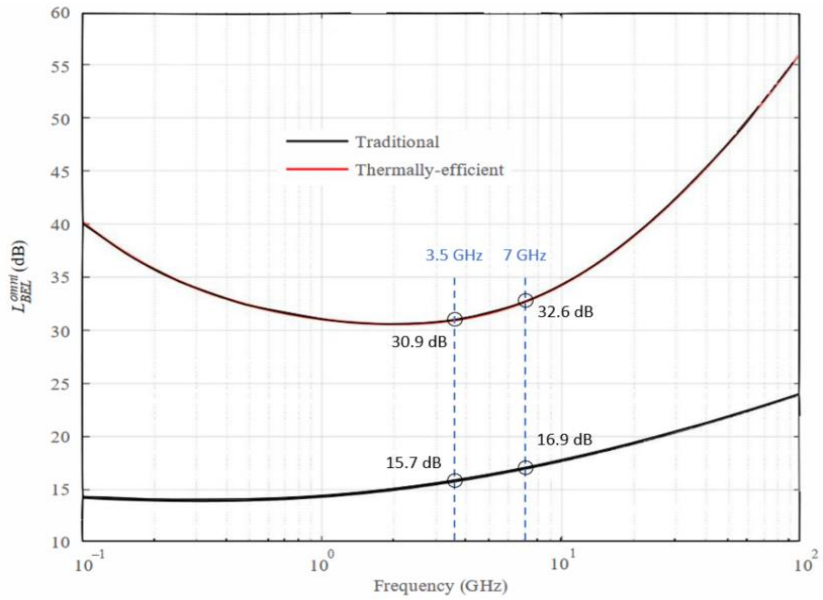

Figure 4 - Median building entry loss versus frequency, as given by the ITU-R P.2109-1 recommendations, with values at 3.5 GHz and 7 GHz highlighted.

Besides, the degradation of outdoor propagation losses in an urban environment can be roughly estimated from the third-generation partnership project (3GPP) UMa path-loss model [[12], section 7.4.1], which is given for frequencies between 0.5 GHz and 100 GHz. Figure 5 shows the evolution of the mean path-loss in line-of-sight (LoS) or non-LoS (NLoS) situations at both frequencies 3.5 GHz and 7 GHz. The difference equals 6 dB. This is obviously a critical degrading factor, which imposes the system to be deployed with a much favourable link budget (e.g. due to the antenna gain), highly improved spectral efficiency and/or higher density. If all parameters of a system are constant except the frequency, it may be deduced from Figure 5 that the NLoS coverage quality that is measured at range 5 km for frequency 3.5 GHz, is obtained at range 3.5 km when operating at 7 GHz.

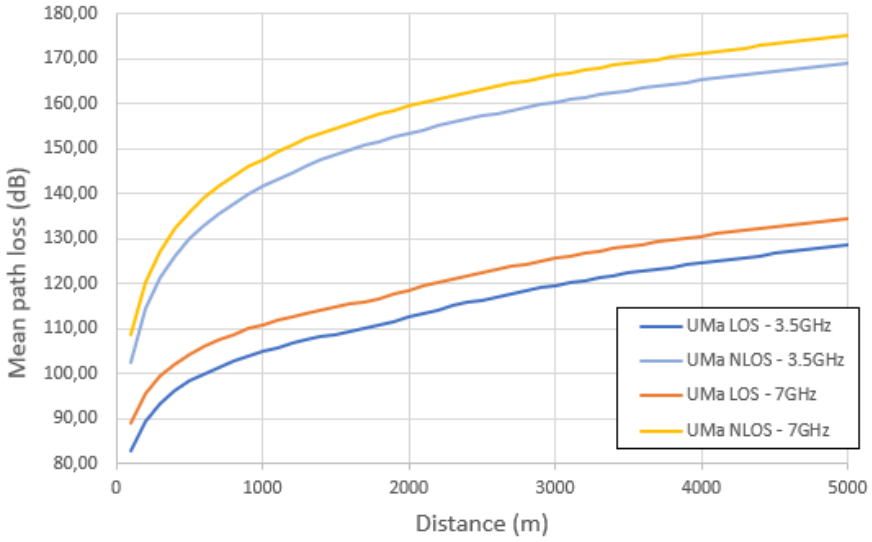

Figure 5 - Mean path-loss vs. distance from the 3GPP UMa model at frequencies 3.5 GHz and 7GHz.

1.4 Network architecture, Open RAN and CF-MIMO

The Radio Access Network (RAN) plays an important role to connect User Equipments (UEs) with the Core Network (CN) accessing services by routing Control Plan (CP) and User Plan (UP) data. Over the different generations of the mobile communication networks, the RAN architecture has been evolved to support new services and applications. The first version of RAN is distributed RAN (D-RAN), followed by centralized RAN (C-RAN), and lastly, virtualized RAN (V-RAN).

In D-RAN architecture, the radio processing and signal processing units of the Base Station (BS) are separated from each other. The radio unit is deployed close to the BS and is called Remote Radio Head (RRH) while baseband signal processing unit is called Baseband Unit (BBU). Each cell site has a BBU a RRH are located at every cell site. They interconnected through a transport network called Front-Haul and each cell site is connected back to the core network through Back-Haul link. To improve the network energy efficiency and resources utilization, C-RAN architecture was developed, where the distributed BBUs are moved into a centralized resource pool at a central cloud server and the RRHs are kept in the various cell sites. Moreover, in contrast to D-RAN, C-RAN splits the BBU functionality into two functional units: Distributed Unit (DU) and Centralized Unit (CU). The DU is the main processing unit that is responsible for the high-physical, Medium Access Control (MAC), and Radio Link Control (RLC) protocols in the RAN protocol stack. The CU runs the Radio Resource Control (RRC) and Packet Data Convergence Protocol (PDCP) layers. In order to lower upfront deployment expenses and operating costs, V-RAN enables the virtualization of the DUs and CUs so that it runs as software on generic hardware platforms. Consequently, processing resources can be shared between various loaded cells which can improve their coordination and simplify network management.

The 3GPP conducted several studies on different possible options for a functional split between the CU and DU to determine differences, advantages and disadvantages of placing different processing units in different locations of the RAN. Consequently, the 3GPP has defined eight functional split options, as shown in Figure 6, inducing trade-offs between centralization gains and Fronthaul bandwidth requirements.

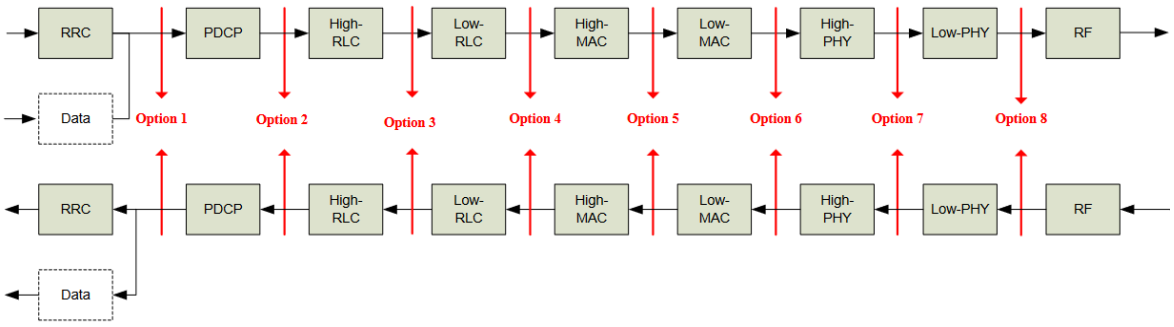

Figure 6 - 3GPP's functional split options [13]

With the evolution of mobile networks looking beyond 5G, the transformation of RAN architecture is required to support heterogeneous services, coordination of technology enabling multi-connectivity, and on-demand deployment of service. 3GPP and O-RAN Alliance are promoting technology standardization, called Open RAN, for the purpose of making the radio access network open,

virtualization and intelligent. The ambition is to enable open and interoperable multi vendor's hardware and software components. Through a process of disaggregation, O-RAN alliance adopted Split option 7-x which splits the physical layer (PHY) into high-PHY and low-PHY, as depicted in Figure 7. Moreover, it defined three distinct components that align with 3GPP Release 15 and beyond: (**a**) the Open-Central Unit (O-CU), (**b**) the Open-Distributed Unit (O-DU), and (**c**) the Open-Radio Unit (O-RU).

In accordance with the 3GPP Next Generation RAN (NG-RAN) and its evolution O-RAN, in POSEIDON project, we propose to disaggregate the classical cell-free massive MIMO central processing unit (CPU) in O-DU and O-CU units. As shown in Figure 7, the O-RU units are located at AP and incorporated the Low-PHY layer and RF processing based on a lower layer functional split. O-RUs are interconnected with the O-DUs through Fronthaul connections, the Midhaul refers to the link between the O-DUs and the CU, and the Backhaul refers to the part of the network that connects the open RAN to the core mobile network.

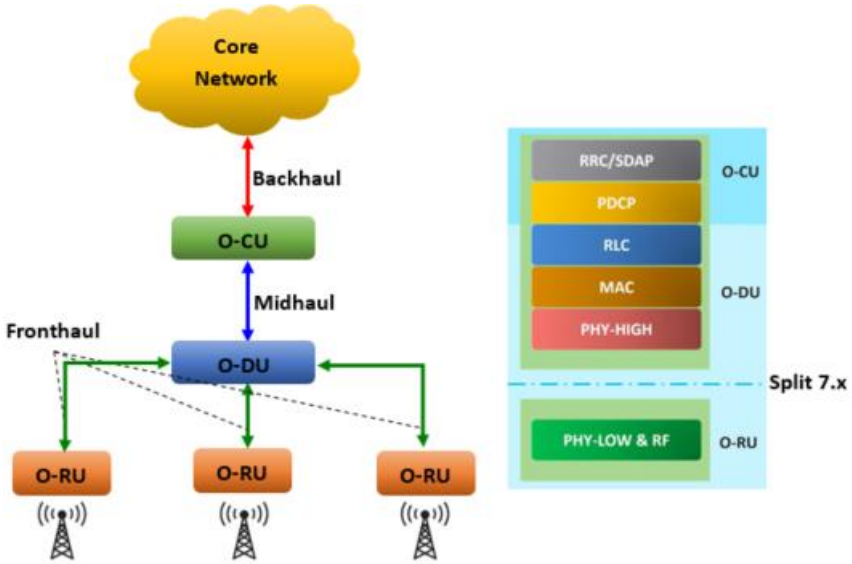

Figure 7 – Logical architecture considered in Open RAN architecture and associated Split 7.X options

The CF-mMIMO concept seems particularly suitable to open RAN architecture Split option 7-x deployment where O-RUs can be jointly controlled by O-DU for joint processing which is relevant to POSEIDON project.

For the Fronthaul network topology, a special attention will be devoted to star and tree with low serialization level topologies. In star topology (Figure 8.a), all the APs (O-RUs) are connected directly to the O-DU which is the easiest solution for joint processing. However, the number of O-RU connections in the star topology is limited by the number of O-DU interfaces. In tree topology (Figure 8.b), the Fronthaul architecture combines characteristics of chain (i.e. bus) and star topologies. The tree topology was highly promoted by researchers with respect to technical-economic feasibility of cell-free massive MIMO systems [14].

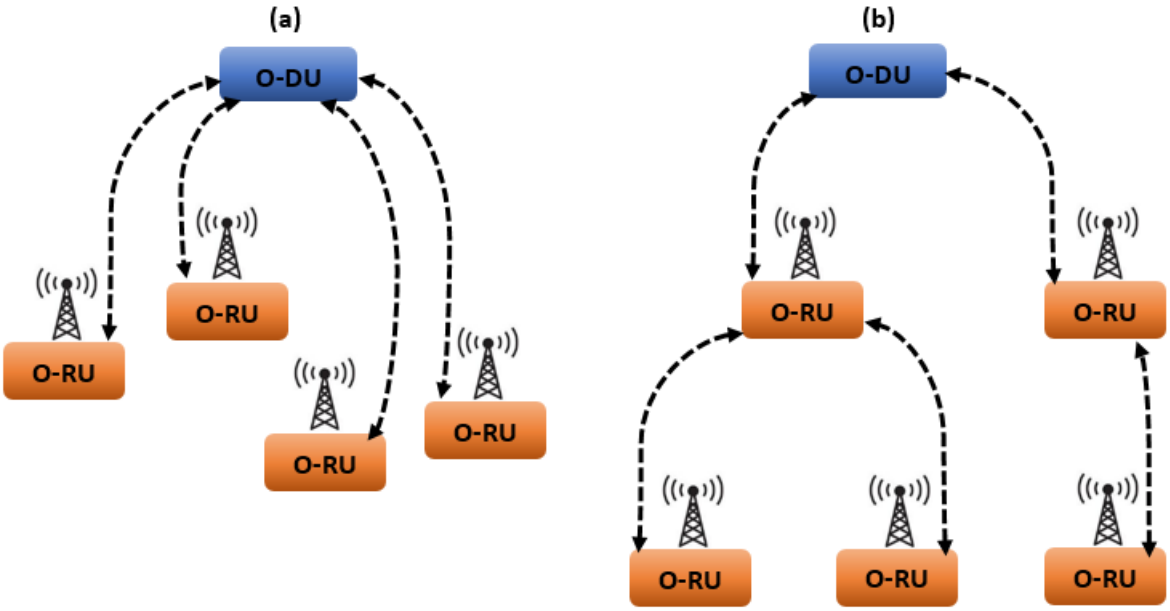

Figure 8 – Fronthaul topologies: (a) Star structure and (b) Tree structure

Multiple options to implement CF mMIMO in the current or possible future O-RAN generations are envisaged and recently studied ([3 – section 3.2.4.3 D-MIMO support in the ORAN] [15] [16]). In a nutshell :

- Current O-RAN architecture supports Cell-Free networks not requiring the Inter-O-DU interface. [15]
- Inter-O-DU interface should be specified in O-RAN in order to enable Cell-Free networks offering high Spectral Efficiency. [15]
- In a user-centric approach combined with local processing, the precoding/combining vector is preferably implemented in the O-RU or O-DU.

2 Uses case, definition and requirements

2.1 eMBB ultra dense network

2.1.1 Introduction

Nowadays, the gains, compared to being deployed 5G network, brought by cellular massive MIMO at 3.5GHz will guarantee a good hold on the traffic increase in the next years. Nevertheless, this solution, which is based on large antenna systems, is only slightly scalable due to the size of the antennas and the space/weight constraints. The design of new solutions exploiting the spatial diversity and the full power of MIMO techniques is therefore necessary.

Moreover, as the propagation of millimeter waves for 5G is limited ("mobile on the move" applications with outdoor/indoor, indoor/outdoor coverage and mobility), a complementary solution bridging the gap is needed. The communication technologies in the centimeter band seem to be the most suitable for the most demanding applications benefiting from both bandwidth and scalable spatial multiplexing with distributed MIMO network. The combination of both cm-wave broadband and large distributed MIMO systems is therefore considered as a key enabler for 6G.

Last but not least, the capability of the current deployments to deal with traffic variations is not completely covered by 5G. So, for these ultra-dense/ultra-broadband applications, the deployment of a technology allowing to limit the exposure, to deploy energy efficient systems is required. We aim to evaluate the gains that can be obtained by the deployment of a promising technology which is the CF-mMIMO

In brief, all the considered parameters are summarized in Table 1 to define the eMBB use case.

Table 1: Parameters for eMMB scenarios

Scenario	Environment	Indoor/Outdoor
	Network coverage range	1-2 km²
	Service	eMBB, Video DL/UL, XR/VR
	Mobility	Pedestrian/low mobility
	Link visibility	LoS/NLoS
	Number of APs	50-200
System & performance requirements	Frequency band	6-7 GHz TDD
	Bandwidth	Up to 100 MHz
	AP Tx power	20-30 dBm
	AP antenna array	8/64
	UE antenna array	1/4
	TDD	Symmetric UL/DL
	Waveform	OFDM 5GNR, Fs=122.88MHz, ICS 30KHz (u=1)
	Modulation	Up to 256QAM

2.1.2 Deployment strategy

The 3.5GHz licensed band supports the main success of the 5G technology; therefore, the mobile operators will firstly look for new technologies that allow the performance of the existing network to be reinforced and not a complete and irreversible swap to new networks. For easy and safe transition between the existing 5G network and the new cell free mMIMO system, we consider the new system as a complementary densification solution to offer offloading capabilities for the eMBB traffic.

Therefore, the eMBB deployment studies will start by considering a macro-cell 5G deployment, which may be inspired from already operational 3.5 GHz public 5G networks (in terms of density, sectorization, etc). This initial macro-cell deployment will have different possible exploitations in the POSEIDON studies:

1- Host a traditional cellular mMIMO network, which is used as a reference configuration for performance comparison purpose;
2- Host the macro layer in an heterogeneous cell-free mMIMO network that is composed of macro and micro APs;
3- Host a cellular mMIMO network, which is completed with a cell-free mMIMO composed of homogeneously distributed micro APs for offloading purpose.

Unlike the macro antennas deployed mainly on buildings' rooftops, the micro APs are expected to be deployed with higher density on top of lampposts, on façades and low building rooftops, and with acceptable size as it must not be heavy and cumbersome.

Two implementations of the eMBB use case are proposed: 1) a theoretical setup i.e. based on analytical models at the physical layer; 2) and a digital twin that relies on a real environment and some physical models.

2.1.3 Theoretical setup

The theoretical setup will be utilized for initial research studies carried out in work-packages WP2 and WP3. Since this setup relies on analytical propagation models and simple deployment rules, it will be possible to derive the network performance in a mathematically tractable way.

The use case is implemented as a 1 km² dense urban area, where all considered mobile users are supposed to be located. If needed for a more accurate performance prediction, a larger area may be considered that includes all interfering base-stations. The path-loss between the base-stations and the mobile users is computed by the 3GPP UMa model for macro base-stations, while the 3GPP UMi model is used for small-cells [17, table 7.4.1-1]. The wideband channel properties, i.e. multi-paths, angles of departure, angles of arrival, and delays, which are useful for estimate of the MIMO coefficients, are given by the 3GPP Clustered Delay Line (CDL) model [17, section 7.7.1].

Macro APs' typical height is 25 meters and micro APs typical height is 10 meters. Mobile users are assumed to be located at ground level, i.e. at1.5 meter high.

The macro APs are uniformly distributed along a hexagonal grid. The inter-site distance for the initial 5G network at 3.5 GHz is supposed to be around 400 meters. The micro APs and mobile users are uniformly distributed in space.

2.1.4 Digital twin setup

The digital twin setup will enable to assess the system performance in a more realistic context, including operational antenna deployments, physical propagation losses and channel properties, and realistic user distributions.

The digital twin setup will also be constructed from a 1 km² area in Paris. Figure 9 shows the 3D map data model which is used to compute realistic wave propagation based on ray-tracing and properly evaluate the coverage and capacity of the studied network. This area represents a typical dense urban environment in Paris (part of the 9th and 10th arrondissements); it is characterized by:

1- Uniform building's height around 20 meters;
2- Mix of high density of small streets and few larger streets/boulevards;
3- Presence of a hotspot area close to Gare du Nord.

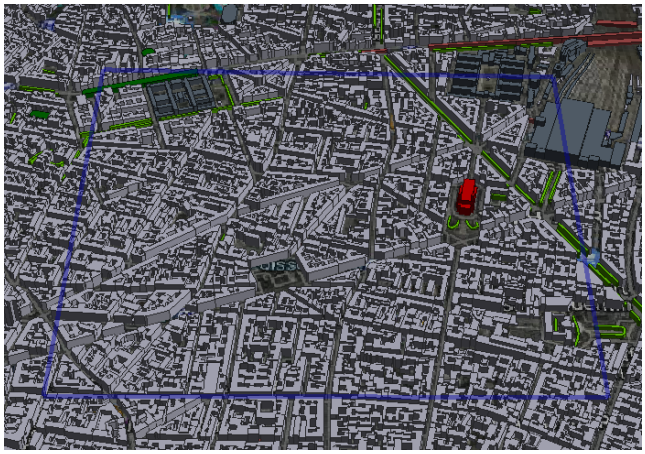

Figure 9 - 3D urban environment modelling

Figure 10 - Google Earth pictures from the considered urban environment.

In order to account for realistic interference, we must consider an interference/buffer area of 10 km² in the simulation (the red square in the figure below). The macro base-stations present in this red area will be integrated in the calculation of the interference to avoid any bias due to the border effect.

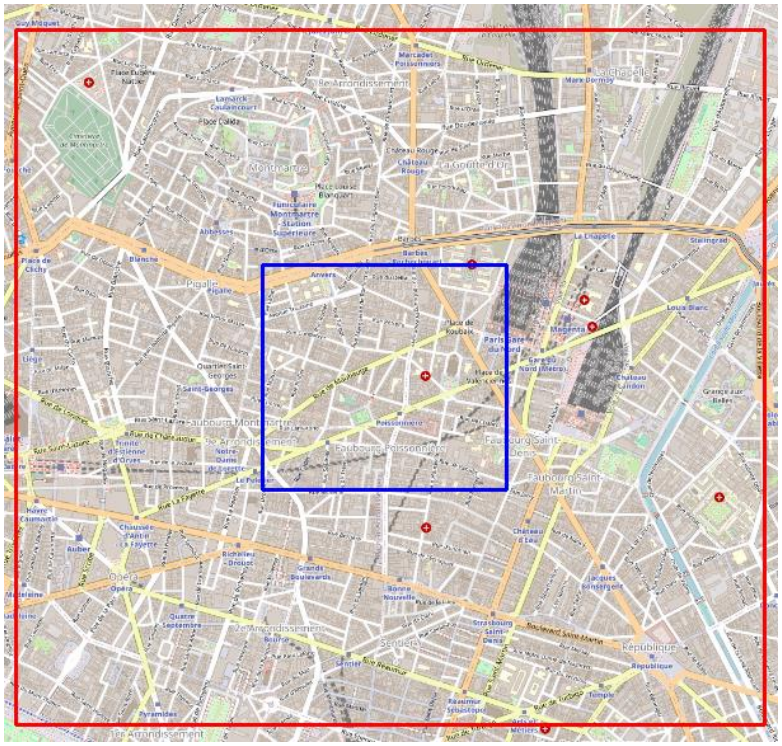

Figure 11 - Area of interest (in blue) and buffer area (in red) for urban simulations.

The initial macro layer will be inspired from an existing 5G deployment by a French mobile network operator. The regulator's website www.cartoradio.fr allows extracting information about the deployed radio access technology, frequency, GPS position, height, and azimuths. In the example shown in Figure 12, we count 49 antennas deployed either in the area of interest or pointing towards it.

Based on the digital twin, the micro APs will be deployed along the streets, mainly positioned on lamppost. In a first stage, a quasi-homogeneous deployment will be realized, controlled by an average inter-site distance. For more accurate evaluations, in a later stage, the SIRADEL automatic cell planning tool (ACP) will select the best AP positions (from a large list of candidates) to maximize the situations with favorable propagation (e.g. line-of-sight LoS) and optimally consider the cell-free requirements in terms of coverage and AP connection diversity.

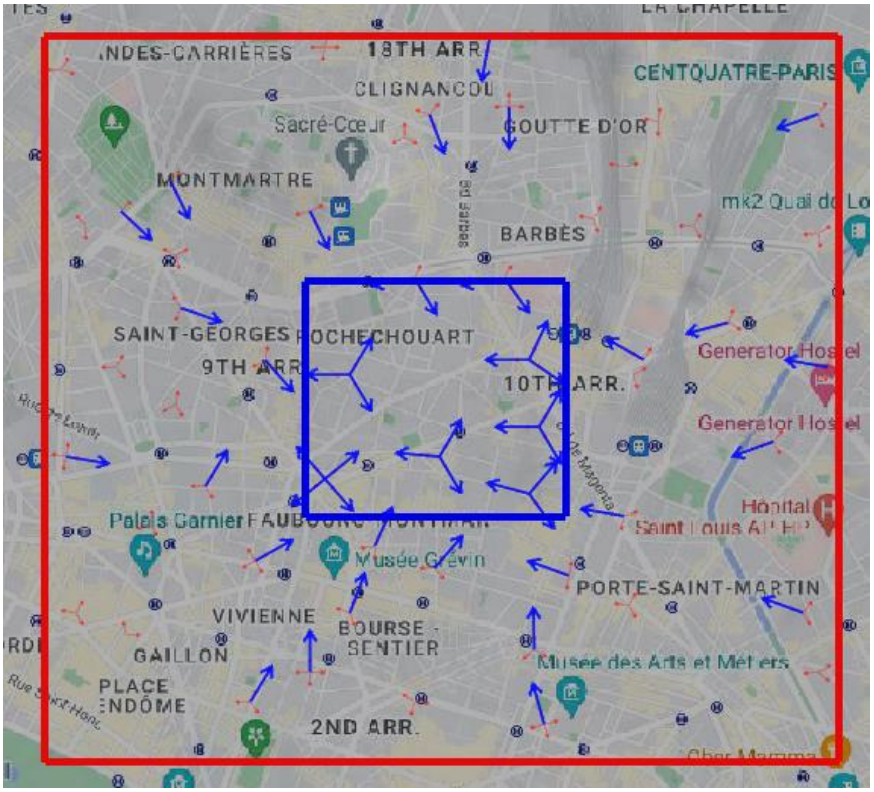

Figure 12 - Real 5G cellular mMIMO network in Paris

2.1.5 Radio configuration

- Frequency band & frame configuration

As cell free mMIMO systems are supposed to coexist with cellular mMIMO systems, we propose to study the deployment of the cell free system at a frequency band complementary to legacy 4G/5G bands with a constraint of global standardization of a spectrum: The 6-7 GHz range can be a promising candidate as cm-wave frequency bands combine high capacity (thanks to MIMO) with good coverage and it is available in most markets [18]. It terms of practical installation concerns, this frequency band is also recommended as the physical radio head size with a large number of antenna elements remains relatively small.

Table 2: System parameters for the eMBB scenario.

Parameters	Value
Frequency band (MHz)	6000
Duplexing mode	TDD
DL/UL ratio	Symmetric (1:1)
Bandwidth (MHz)	100
Numerology (μ)	1
#PRBs	273
Slot duration (ms)	0.5

In order to lead a fair comparison and analysis between existing systems and the new cell free technology, we consider the same configuration as 5G in 3.5 GHz in terms of possible numerology (we fixed it to 2 for both control and data traffic), duplexing mode (TDD), bandwidth (100 MHz).

- Base Station (BS) / Access Point (AP) configuration

The macro base-stations (in cellular network) and macro APs (in cell-free network) are supposed to be deployed on tri-sectorial sites. The antenna array of a cellular BS is considered to be formed by at least 64 elements (128 elements may be a typical value), while the size of the cell-free APs antenna is in range from 8 to 128 elements. The antenna elements are uniformly distributed along a rectangular or square vertical panel. Dual-polarized antenna elements are preferred; but single-polarized radiation can be considered as well for simplification in some studies. The distance between two antenna elements is preferably $\lambda/2$.

The radiation pattern of each antenna element is directive with a 3dB-beamwidth of 60°-65° in the horizontal dimension. The analytical antenna model proposed in [17, section 7.3] can be used.

Operational antenna representations, provided by 5G antenna manufacturers, can be integrated in the Digital twin setup. For instance, Figure 13 shows an example of a single sideband antenna pattern used by existing 5G cellular tri-sectorial mMIMO systems. The strong antenna gain (25 dBi) is obtained by the beamforming built from a very large antenna array (up to 128 elements). Such high-gain directional antenna will be considered for simulation of the baseline 5G network coverage.

Even smaller antenna arrays will be considered for the micro AP's, i.e. between 8 and 64 elements. The directivity of the radiation pattern (65° aperture, omni-directional, other) will be decided depending on the studied deployment strategy, the installation constraints and capacity requirements.

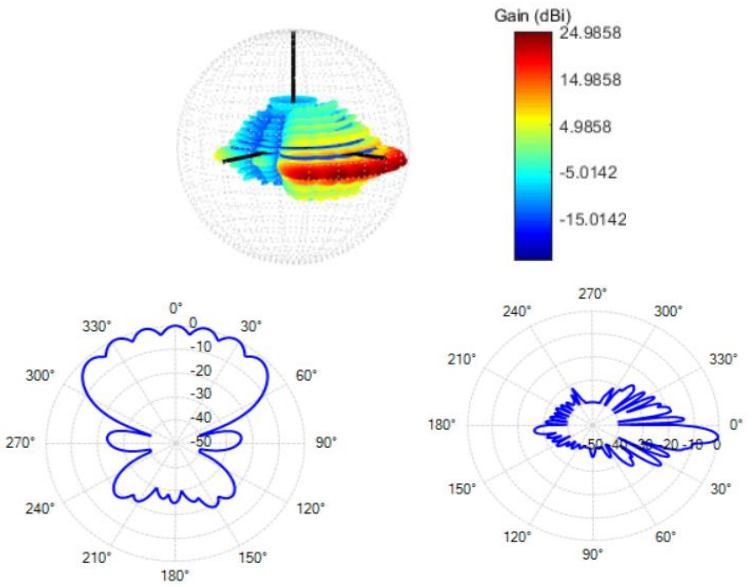

Figure 13 - Example of a 5G antenna radiation pattern used at the macro bases-stations

- User Equipment (UE) configuration

Recent 5G smartphone models in the market are equipped with 4x4 MIMO antennas which means that they support the 4T4R communication mode (4T4R is a transmit and receive mode where the BS or AP can transmit simultaneously up to four data streams to one UE). For this reason, we consider that UE can be equipped by a maximum of 4 antennas and supports multi-stream transmission with up to 4 streams per user.

It may be possible to include data traffic maps in this scenario as the UE distribution must be heterogeneous between indoor and outdoor and also in crowded streets, attractions, etc.. In case indoor users have to be considered, it can be assumed that 80% users are located inside buildings [17, table 7.2-1].

2.1.1 Preliminary coverage results

In this section, we provide initial coverage results in the digital twin setup based on the described scenario with the real 5G cellular mMIMO network in the study area in Paris. Figure 14 depicts the RSRP (Reference signal Receive Power) map of two equivalent deployments: one at 3.5GHz, the other at 6GHz.

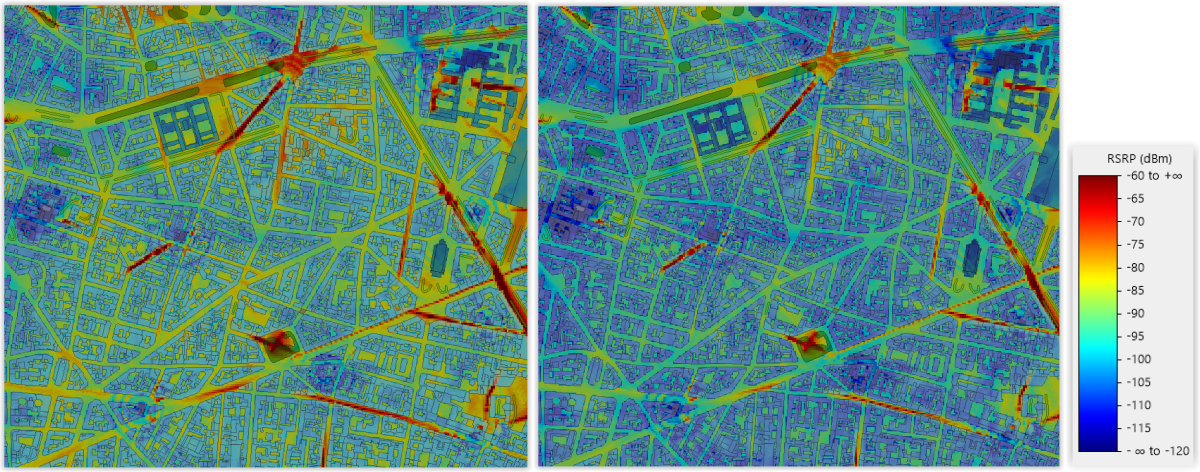

Figure 14 - RSRP map at 3.5GHz (left side) and 6GHz (right side)

As one would expect, we can observe in Figure 14 that the coverage is better at 3.5GHz than at 6GHz (on average more power received at 3.5GHz). The Figure 15 illustrates the difference in received power between the two considered frequency bands in this scenario and we observe again the behaviour of signal degradation when switching from 3.5 to 6 GHz transmissions. Furthermore, considering 3.5GHz links instead of 6GHz reduces the propagation attenuation by about 6 dB for both LOS and NLOS situations. This is in accordance with the propagation analysis given in subsection 1.3.1.

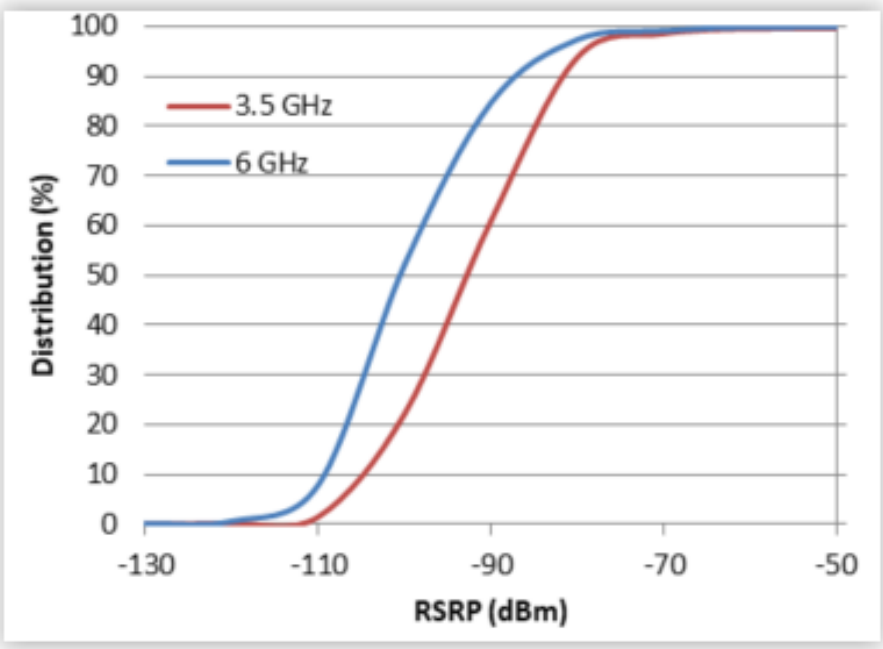

Figure 15 -RSRP CDF distribution for both frequency bands 3.5 and 6 GHz

For instance, at 3.5 GHz, more than 75% of covered pixels have a received signal higher than -100 dBm. However, at 6 GHz, only less than 50% of covered pixels can reach a reception higher than -100 dBm.

2.1.2 Target application and the related KPI requirements

In beyond 5G technology, the new main ultra eMBB applications or use cases dedicated to the general public are potentially 4K video streaming, extended reality (with its three main immersive features which are Augmented Reality, Virtual Reality and Mixed Reality) and holograms. The KPI requirements for these use-cases are presented in the table Table 3.

Table 3: KPI requirements for the eMBB scenarios [20][21][22][23][24].

KPI\Use case	4K video streaming	Extended reality	Holograms
Peak data rate (Mbps)	1000	1000	2000
Experienced data rate (Mbps)	100	50	300
Reliability (%)	99.9	99.999	99.999
Availabilty (%)	99.9	99.999	99.999

2.1.3 Target studies

The eMBB urban scenario is always a major target to evaluate the efficiency of a new mobile network technology. We consider this scenario to realize the following main studies:

- Characterization of correlation levels in channel matrices of CF-mMIMO LOS/NLOS channels and evaluation of the relevance of the Gaussian model widely considered in the literature.
- Performance assessment of channel estimation, novel precoding scheme with realistic propagation environment combined with transceiver hardware impairments.

- Performance comparison to conventional co-cellular mMIMO network in order to better identify the situations and configurations where the cell-free technology outperforms existing 5G technologies in terms of classic technological KPIs such as capacity, but also in terms of energy efficiency and electromagnetic field (EMF) exposure. It may be possible to compare the performance of cell-free systems to other densification topologies such as the use of relays or reconfigurable intelligent surface (RIS).
- Optimization of AP density, antenna size and transmitted power with the aim to reach the optimal performance of the cell-free system mainly in terms of capacity and coverage and at the same time reduce the energy consumption.
- Evaluation of the required fronthaul capacity in order to design a viable and scalable system. In this scenario, we consider that the fronthaul medium is composed of a fiber network complemented by sub-THz in subareas where fiber is not accessible. The sub-THz fronthaul design will be made following a mesh topology and considering redundancy requirements to be connected to only one centralized/virtualized CPU (which is in line with the emergence of ORAN technology). It is important to note that the sub-THz fronthaul will impact the positioning and the density of the cell-free APs.

2.2 Multi-service Private network

2.2.1 Introduction

The deployment of private mobile networks is expected to completely transform several industries (such as factories' automation and the transportation and logistics sectors) and will have a major impact on how they function. In addition to MEC (Mobile Edge Computing), TSN (Time-Sensitive Networking) and security enhancements, CF-mMIMO technology is also expected to improve the required availability and reliability of communications in indoor environments such as factories as it increases the LoS coverage and reduces the probability of blockage (each user can be served by several APs).

Through this proposed private network scenario, we aim to identify the possible gains that can be generated from using the cell free technology in a private indoor environment.

2.2.2 Deployment strategy

In terms of infrastructure, we will study the deployment of a standalone private network. In other words, the main coverage is provided by the PMR (Professional Mobile Radio) network and UEs switch automatically from the public network once they are in the coverage of the PMR network. One of the main advantages of deploying a dense cell-free topology is the increase in LOS coverage and thus significant improvement of the radio conditions and link availability. The constructive combination of diverse radio links should greatly improve the reliability.

A dense PMR infrastructure can also be very beneficial for positioning purposes; However this won't be directly studied within the POSEIDON project.

2.2.3 Theoretical setup

CF-mMIMO systems is expected to be a promising solution for small-scale PMR networks, where obstacles like walls, bulky furniture or metallic partitions can make the propagation conditions difficult. They can be deployed in a factory, a shopping mall, an airport or a train station. The main objective is to reduce NLOS situations and improve connectivity all over the covered area.

One private network scenario that will be tested in POSEIDON is a factory where empirical propagation models as well as simplified deployment constraints can be considered; and where mathematically tractable approaches can be derived.

The indoor factory scenario (InF) of the 3GPP channel model will be used. Five different factory layouts are proposed [17, table 7.2-4], with various sizes (up to 160 000 m²), several ceiling heights (up to 25 m) and different clutter definitions (e.g. big/low machinery, low/high machinery density). The associated path-loss model and the LoS probability are given respectively in [17, table 7.4.1-1], [17, table 7.4.2-1]. The simple CDL channel model described in [17, section 7.7.1] can be scaled from the inF channel statistics like delay and angle spreads given in [17, table 7.5-6].

2.2.4 Digital twin setup

In the digital twin, we consider a detailed environment in a factory of size 21,000 m², for which the partners already have the 3D digital model. As shown in Figure 16, the factory is composed of three main zones each with different shapes, sizes, materials, and clutter density. We find in zone A metallic machines and metallic storage containers. Zone B is almost empty for the purpose of movement of factory workers transporting factory loads. Zone C contains metallic lockers and wooden benches and some metallic housing units.

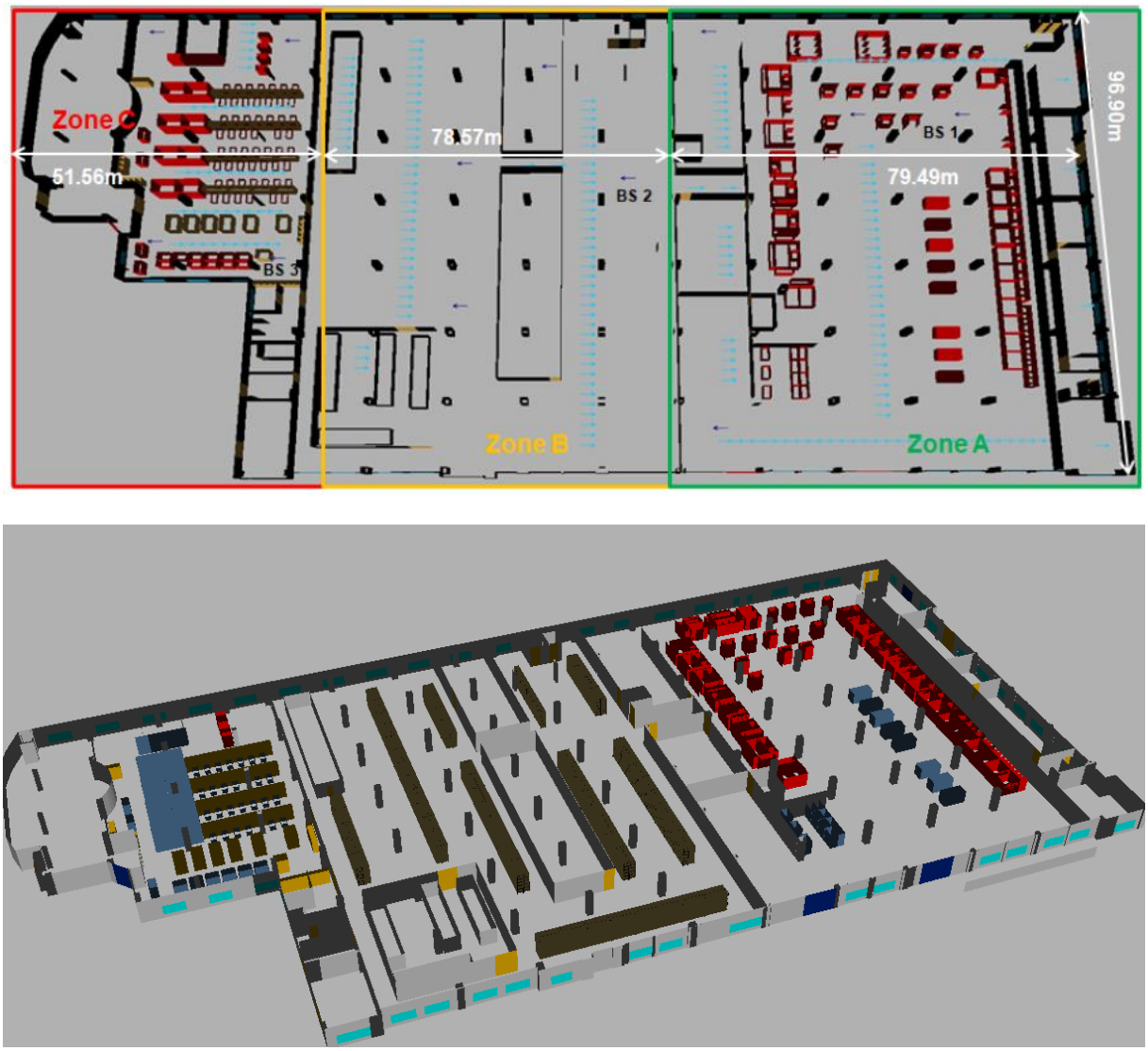

Figure 16 - 3D factory model.

We propose an extra PMR scenario that will be addressed in best effort mode (i.e. we cannot guarantee this scenario will be studied). The scenario concerns a well-known train station in France which is “Gare du Nord” in Paris, the first station in Europe and the third in the world in terms of number of passengers with more than 220 million of visitors per year.

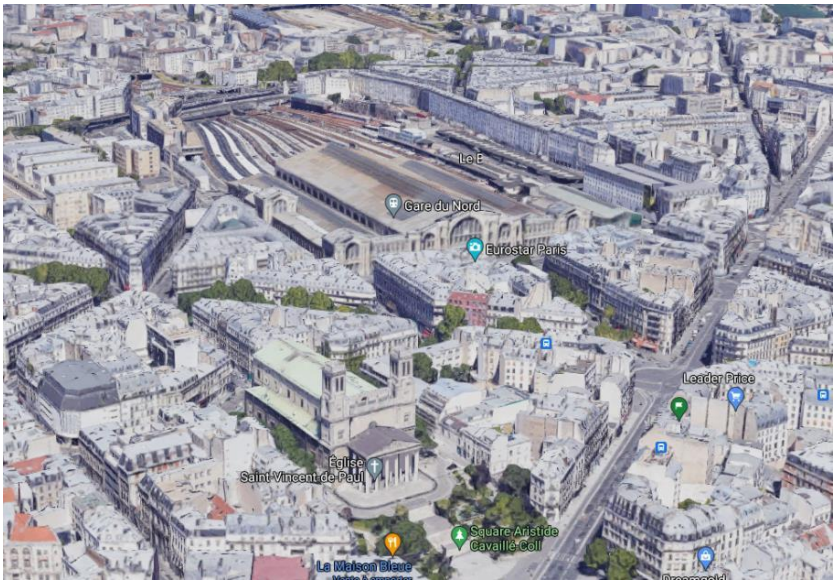

Figure 17 - Environnent of the "Gare du Nord".

The station and its surroundings are finely modeled in the digital twin to properly simulate the propagation signals. Figure 18 illustrates the 3D map data of the study area.

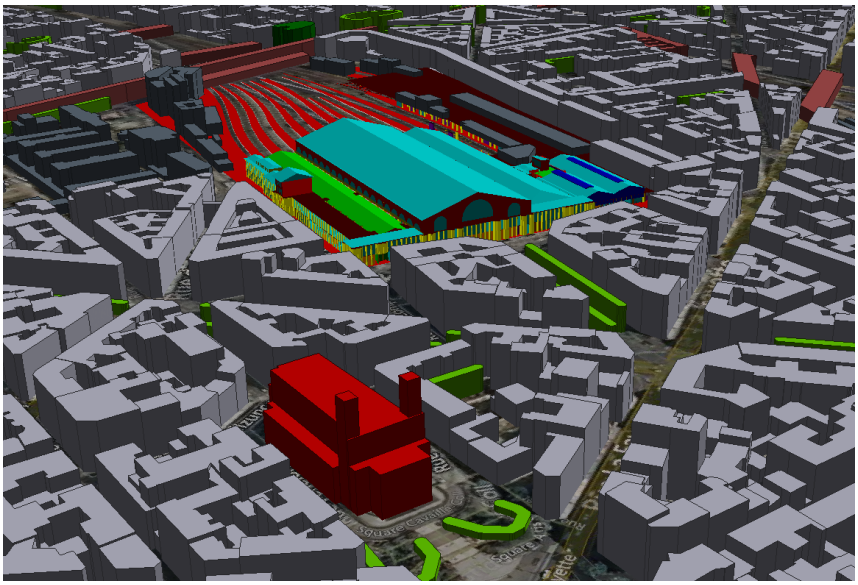

Figure 18 - 3D digital model of the "Gare du Nord".

The study area is a mix of different shapes, sizes, materials, and clutter density. To simulate realistic obstructions, the materials' properties are also finely defined (different layers of the map data can be distinguished in Figure 19).

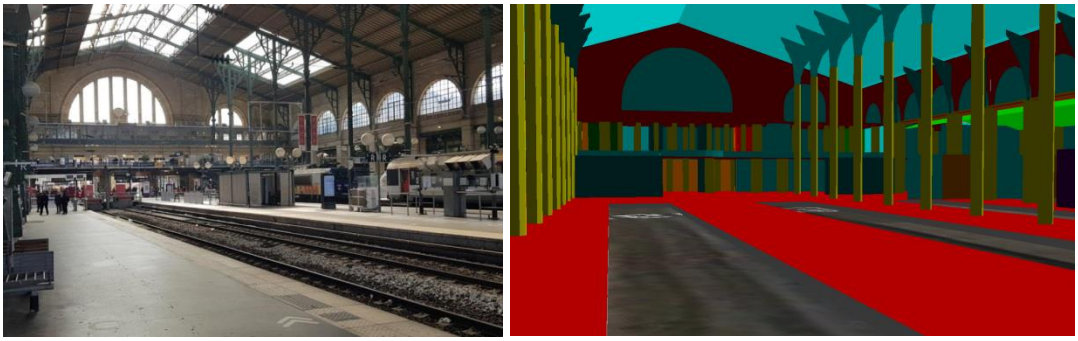

Figure 19 - Interior of the “Gare du Nord” environment.

2.2.5 Radio configuration

- Frequency band & frame configuration

The C-band (between 3.7 and 4.2 GHz) is widely used in private network deployments [19]. It provides an optimal balance between coverage and capacity for cost efficient implementation. The PMR scenarios are very challenging especially because of either the high density of connected devices or the high reliability requirements. Therefore, considering the C-band can be a relevant solution for high capacity and reliability demanding scenario as it will provide more spectrum availability. The rest of the parameters considered in this scenario are summarized in the Table 4.

Table 4: System parameters for the private network scenario.

Parameter	Value
Frequency band (MHz)	3700-4200
Duplexing mode	TDD
DL/UL ratio	Symmetric (1 :1)
Bandwidth (MHz)	100
Numerology (μ)	1 or 2
#Prb	273 or 135
Slot duration (ms)	0.5

- Access Point (AP) configuration

The APs are equipped with up to 16 antenna elements and transmits a max power between 20 and 30 dBm. The choice of the antenna directivity (horizontal aperture 60°, or 90°, or omni-directional) will depend on the installation e.g., an omni-directional antenna can be used for APs installed below the rooftop in the middle of a room, while a 90° directional antenna is preferred for APs installed against walls. Multi-sectorial APs could be also deployed for high-capacity scenarios, but it is quite unlikely.

- User Equipment (UE) configuration

In this scenario, the simplest UE devices like sensors are equipped with a low-complexity low-power radio-end; we may suppose that they have only 1 or 2 antenna elements. The other UEs are equipped with maximum 4 antenna elements and hold the same capabilities described in the previous scenario. Various mobility levels up to 30 km/h can be integrated in the simulation scenarios e.g.:

- Fixed sensor: 0 km/h;
- Pedestrian: 0 to 3 km/h;
- AGV (Automated Guided Vehicles), robot, drone or forklift: 30 km/h.

2.2.6 Target application and related KPI requirements

The PMR network in the factory scenario is expected to offer different types of services with heterogeneous KPI requirements. The PMR network must cover:

1. Telepresence and mixed reality applications where high capacity and data rates are required,
2. Remote control of robots and UAVs where low latency and high reliability are mandatory,
3. Sensors: high availability requirement and high density of connected equipment but with sporadic traffic and low required data rates.

The corresponding KPI requirements are illustrated in Table 5.

Table 5: KPI requirements for the private network scenario [20][21][22][23][24].

KPI/USE CASE	Telepresence and MR	Remote Control	Sensors
Peak Data Rate (Mbps)	1000	100	0.1
Experienced Data Rate (Mbps)	50	10	0.01
Reliability (%)	99.9	99.9999	99.99
Availabilty (%)	99.9	99.9999	99.99

2.2.7 Target studies

The PMR scenario is the second major scenario to evaluate the efficiency and the gain of deploying the cell-free technology. We consider this scenario to realize the following main studies:

- Performance assessment of channel estimation, novel precoding scheme with realistic propagation environment combined with hardware impairments.
- Performance comparison to conventional co-cellular mMIMO network to understand how CF-mMIMO technology can improve the actual 5G system performances.
- Define new design rules and recommendations for PMR network deployments using the cell-free technology.
- Evaluation of the required fronthaul capacity to design a viable and scalable system. In this scenario, we consider that the fronthaul is either completely fibered or partially fibered and complemented using IAB operating at the same access frequency band of 3.7 GHz. Note that in case we consider IAB, the APs deployment will be highly impacted with the IAB constraints.

2.3 Vehicular to Infrastructure (V2I)

2.3.1 Introduction

The realm of vehicular communications is rapidly expanding in two different directions. Firstly, it involves the pathway to autonomous vehicles, including the advancement of ADAS (Advanced Driver Assistance Systems) and the exchange of information and data fusion, which necessitates a high level of service quality. Secondly, there is a focus on entertainment, whereby vehicles are transformed into hubs for passengers to consume digital content.

Regarding ADAS, vehicles are equipped with numerous sensors and equipment that ensure safety. These sensors and devices interact with the environment and collect significant amounts of data, which is then utilized to regulate the acceleration and speed of the vehicle.

The implementation of intelligent transportation systems is a means to mitigate the effects of traffic congestion and enhance safety. By automatically coordinating and controlling vehicles, these systems can increase the capacity of highways and create platoons, which are groups of vehicles that travel in close proximity to one another. Challenges faced are delays and interference, which are caused by many factors. In order to facilitate effective communication through Vehicle to Interface (V2I), it is crucial to minimize delays and interference. Prolonged delays can have a negative impact on the performance metrics of a positioning terminal, which are typically measured in terms of accuracy, availability, and integrity.

A distributed MIMO network has the potential to offer an effective solution to the challenges of managing interference and ensuring consistent signal quality across all areas. This is achieved through the use of multiple antennas and spatial processing techniques, which can enhance signal reception and mitigate interference between various users or devices within the network.

Again the combination of distributed massive MIMO system and new frequency bands (cm) seems to be a key enablers for 6G intelligent vehicle network. In brief, all the parameters envisaged are summarized in Table 6 to define the V2I use case.

Table 6: Parameters for V2I scenarios

Environment	OUTDOOR
Network coverage range	100-200 km (motorway)
Services	MTC, URLLC, eMBB
Mobility	Up to 140 km/h
Link visibility	LoS/NLoS
Number of devices/km	200
Number of AP/km	1-5
Frequency band	6-7 GHz TDD
Bandwidth	100 MHz
Tx power	30 dBm
BS antenna array	8/64
UE antenna array	2/4
TDD	Symmetric UL/DL
Waveform	OFDM 5GNR, Fs=122.88 MHz, ICS 30/60kHz (u=1,2)
Modulation	Up to 256QAM

Despite the fact that 5G-NR Vehicle-to-Everything (V2X) provides advanced services, this improvement is the result of increased investment in spectral and HW resources, while still utilizing the underlying mechanisms and system architectures of LTE-based V2X. In addition, due to urbanization and technological advancements, the number of autonomous vehicles is expected to grow rapidly in the future. The growth of intelligent autonomous vehicles is expected to fuel a significant increase in the use of communications devices and digital applications. Moreover, 6G is expected to support all types of high mobility communications, e.g., with a speed up to 500km/h. Hence 5G communications will have numerous applications in high-mobility scenarios, including automotive, high-speed trains and aviation use cases. In general, high-mobility communication is not only about how high is the maximum speed, it is more about the challenges caused by mobility (channel aging, resource management, efficient handover, ...). In order to provide high mobility support to 6G, there are a number of technical issues to be investigated. This includes advanced signal processing for PHY/MAC operations when high mobility is involved, transceiver structures that can exploit the properties of high mobility environments, signal processing techniques that can mitigate the impairments in high-mobility environments, efficient mobility management, and new network architectures.

2.3.2 Target application and the related KPI requirements

The vertical industry in focus is the automotive sector. 6G systems are considered as the main drive of acceleration of development of V2X ecosystem, due to better performance in terms of tackling the main high-mobility issues and handling ultra-dense traffic environments, the features being in line with core motivations of V2X, i.e., improving road safety, traffic efficiency, and energy saving. These motivations are planned to be achieved by building the extensive Intelligent Transport System (ITS) allowing smart and efficient road service for users, acquiring, sharing, and using the information to support individual actions.

2.3.3 Theoretical setup

For evaluation, the 3GPP Rural Macro (RMa) channel model will be used. The rural deployment scenario focuses on larger and continuous coverage. The key characteristics of this scenario are continuous wide area coverage supporting high-speed vehicles. This scenario will be noise-limited and/or interference limited, using large transmit power. The access point height is 35 m. Path loss models are defined in [17]. For our evaluation, only LOS channels will be investigated.

2.3.4 Target studies

This scenario will not benefit from as detailed an implementation as the first two. Nevertheless, it is of particular interest in answering the following research question:

- Grant free, dynamic resource allocation & clustering
- Channel estimation in a fast moving environment, channel aging…

2.4 MTC / Iot

2.4.1 Introduction

5G and beyond 5G mobile systems are expected to provide three core service areas : enhanced mobile broadband (eMBB), ultra-reliable low latency communications (URLLC) and massive machine-type communications (mMTC). Each of these service areas is allowed to exist as a separate network while all three utilize the same physical infrastructure. In the latter case, the available bandwidth is divided across each of these service areas.

The mMTC service area offers low bandwidth connectivity with deep coverage. It helps collect large volume of small data packets from a huge number of devices simultaneously. This technology supports a high density of connected devices. The mMTC network is latent tolerant (latency < 10 s) and supports the transmission and reception of small data blocks over low bandwidth channels. This technology can support up to 1 million devices per square kilometer and has the capacity to afford connected devices around 10 times the maximum capacity offered by 4G LTE. In this technology, data generation, transmission, and actuation take place with nearly zero human intervention. This technology can support machine-to-machine communication without battery replacement for up to 10 years. Most mMTC applications are characterized by the transmission of sporadic burst of short data packets over a relatively long distance (up to 10 Km), low bandwidth, low-power devices and long-life battery or power supply requirements.

One use case includes intelligent agriculture systems, where hundreds of sensors send weather, soil moisture and fill-level data across areas of remote farmland. Other use cases concern traffic management, patient monitoring systems, smart logistics, smart metering, smart homes, smart buildings and smart cities. In the Poseidon project, we focus on the smart city application.

In 1990 just 14% of people on earth lived in cities, but today over 55% of the world’s population lives in urban areas, and the rate continues to grow. It is predicted that by 2050, the percentage of people living in urban areas will edge closer to 70%. Improving cities is thus a pressing global need as the world’s population grows and our species become rapidly more urbanized. Managing the resources and operations of so many large cities can only be cost-effective and efficient if they are automated and connected, which is the basic premise of smart cities.

In a smart city, sensors can be placed everywhere to collect data, with streets, buildings, public and personal devices all being interconnected, and the huge amount of data generated by these sensors then being communicated, analysed and fed back to the infrastructure to affect changes in operation. Example applications can include water, gas and electricity monitoring, waste management, traffic and parking management, logistics and fleet management of public vehicles, environmental sensors for air and water quality monitoring, as well as electronic billboards and charging stations for electric vehicles. In most of these use cases, there are sensors and IOT-based subsystems. An example of IOT devices in the context of waste management could be fill-level sensors on bins that enable waste management teams to only visit bins that need emptying. This would reduce operating costs, save fuel and reduce emissions as waste collection services are targeted to where they are needed. Within smart cities, sensors can be placed strategically around the city to collect data, which is sent back to a central server and analysed to present meaningful information. Different sensors report back different data sets which can be combined to give insight into improvements that can be made. For example, combining

and analysing data from thousands of traffic cameras, radar traffic counters, and air quality sensors could help to reduce traffic congestion and improve air quality for residents in a smart city.

IoT is an emerging paradigm for future communication systems, which has been investigated for co-located massive MIMO systems as massive MIMO can support massive connectivity due to its high capacity, reliability, and energy efficiency. Recently, cell-free massive MIMO was investigated as a way to support IoT systems. By leveraging the macro-diversity gain and better coverage resulting from distributed antennas, cell-free massive MIMO can outperform the IoT network supported by co-located massive MIMO systems. Therefore, it is interesting to consider and further study the use of cell-free massive MIMO to support IoT.

2.4.2 Target application and the related KPI requirements

As mentioned in the previous section, the target application of mMTC area considered in Poseidon is the smart city with the objective to enable massive connectivity, for the uplink, from limited time-frequency resources. The uplink represents a primary challenge due to the massive number of uncoordinated connections in mMTC and is the focused of this part. Current solutions to enable massive connectivity mainly fall into two categories: medium access control (MAC) and physical (PHY) layer solutions [43].

The MAC-layer solutions aim to redesign the access protocols such that the limited time-frequency resource can be shared by more devices. For example, as a new 3GPP technology toward mMTC scenarios, the narrow-band IoT (NB-IoT) standard [44] enables subcarrier-level resource allocation and supports single-tone transmissions with a subcarrier spacing as low as 3.75 kHz, allowing more devices to be serve simultaneously. Another example is the grant-free transmission [45]. Indeed, Grant-based access control requires additional control signalling or message exchanges to facilitate the granting of resources. In mMTC, traffic patterns are partly unpredictable and sporadic due to uncoordinated sleep cycles, making grant-based scheduled access design difficult and potentially inefficient. On the other hand, grant-free access requires only very low control overhead, but often suffers from collisions and low efficiency. However, with an appropriate collision resolution mechanism, grant-free access can be made highly efficient. Consequently, grant-free access control seems favorable for mMTC.

As discussed earlier, random access protocols are strongly affected by collisions, that is, multiple users access a resource concurrently, and thus cannot be successfully detected and decoded. The outcome of collisions, though, is strongly dependent on the specific physical layer technologies. The PHY-layer solutions are mostly based on advanced receiver techniques based on non-orthogonal multiple access (NOMA), including successive interference cancellation (SIC)-based, compressive-sensing (CS)-based multiuser detection or sparse code multiple access (SCMA). SIC arises in power-domain NOMA [46], where multiple signals with power differences can be decoded successively. CS-based methods have frequently been applied to user activity detection for sporadic traffic [47] and data decoding with sparse codebooks [48]. Both SIC and CS methods are applicable for data decoding in the signature-based NOMA schemes [49], where the signature represents the way the data stream of an active device is spread over available resources, i.e., device-specific codebook structures, delays patterns, spreading sequences etc… in a non-orthogonal manner. Consequently, CS-MUD and SCMA targets enhanced resource efficiency and number of served users through non-orthogonal random access in combination with a joint detection of user activity and data.

Finally, the energy efficiency of MTC devices is strongly affected by the amount of overhead seen in the exchange of messages required before the data payload is transmitted successfully. Simply speaking, less frequent and shorter transmissions preserve energy. Therefore, low signalling overhead MAC protocols are one enabler for energy-efficient MTC devices. These types of protocols, coupled with efficient PHY approaches, can then enable devices with long battery lives.

Scenario parameters considered for this part are summarized in Table 7.

Table 7: Parameters for IoT/MTC scenarios

ENVIRONMENT	OUTDOOR
Network coverage range	10-20 km
Services	IoT
Mobility	low
Link visibility	LoS/NLoS
Number of devices/km²	200
Number of AP/km²	1-5
Frequency band	900MHz FDD
Bandwidth	Up to 2 MHz (3.75kHz x 48)
Tx power	23 dBm
BS antenna array	2 (polar)
UE antenna array	1-2 (diversity polar)
Waveform	NB-IoT (single and multi tone)
Modulation	Up to 16QAM – pi/2 BPSK

2.4.3 Theoretical setup

In this study, we outline the setup and scenario for OFDM communication system operating at a carrier frequency of 900 MHz. The goal is to investigate various aspects of the system's performance, including channel characteristics, user distribution, and resource allocation. This scenario is designed to align with the overarching vision of mMTC services.

Signal Parameters:

- The chosen waveform is OFDM with π/2-BPSK modulation.
- Subcarrier Spacing (δf): 3.75 kHz
- Symbol Duration: 2 ms for 7 OFDM symbols
- Carrier Frequency: 900 MHz
- The resource block consists of a 180 kHz bandwidth, accommodating 48 subcarriers, each with a spacing of 3.75 kHz.

User Distribution:

To model the user distribution, we consider a deterministic grid for the placement of access points and a Bernoulli distribution for user association. This approach introduces controlled randomness while ensuring a realistic deployment scenario.

Packet Arrival:

We consider a Poisson arrival process for packets, which will be integrated into the study at a later stage. This stochastic process allows for the assessment of network performance under variable traffic conditions.

AP Clustering:

To explore the effects of AP clustering, we vary the number of APs in a cluster (T = 2, 3, 4, etc.). This variation in cluster size enables the analysis of network behavior in scenarios with different AP densities.

Antenna Configurations:

Both APs and users are equipped with antennas. APs have the option of having one or two antennas (M = 1, 2), while users are equipped with a single antenna. The choice of antenna configurations introduces diversity in the system.

Channel and System Models

- Path Loss Model: We adopt the path loss model as specified by 3GPP standards [25].
- Small-Scale Fading Model: Rayleigh fading is used to model small-scale fading.
- Doppler Effect: For the current study, we neglect the Doppler effect due to very low mobility in the 900 MHz frequency range.
- In a first approximation, we can consider a network without interference, but it may have interfering clusters.
- Spectral Efficiency: The system's spectral efficiency is 0.3 bits/s/Hz.
- AP Placement: APs are deployed in a deterministic grid or random configuration, with a minimum distance constraint between APs if the latter is chosen.
- Maximum Transmit Power: The APs have a maximum transmit power of 23 dBm.
- Noise Power Spectral Density (N0): N0 is set to -174 dBm/Hz.

Validation methodology:

We generate a behavioral system model based on simulations, analytical studies, or a hybrid approach. This model encompasses various aspects, including channel characteristics, resource allocation, and user behavior.

2.4.4 Target studies

For this scenario, we consider a NB-IoT waveform jointly with a grant-free random access protocol such that users are randomly active in the resulting contention period. Due to the random activity in each slot, only a subset of users is actively sending data. From a PHY perspective, this leads to estimation problems with sparsity, as the subset of active users is unknown and has to be estimated jointly with the user data.

The sparsity property of the received signal allows to consider CS-MUD or SCMA techniques to solve the collision problem. To further enhance the connectivity capability of mMTC networks, we propose

to consider, solely or in addition to previous techniques, widely linear processing at reception [50], with its interesting capability to create virtual antennas [51], provided improper modulations are considered. For this reason, we consider pi/2-BPSK modulation, which is permitted by the NB-IoT uplink, which simplifies the NB-IoT user equipment design, assists in coverage enhancement, and is sufficient to support the date rate in the UL. Considering the application of NB-IoT to mMTC scenarios, it is desirable to design mechanisms that can further improve the performance of NB-IoT networks, especially in terms of the number of devices supported per sector. Such a study has been done recently in [52], with very promising results, but for mMTC cellular networks and without exploiting the sparsity of the observations.

We propose to evaluate the applicability of the existing grant-free random access scheme, developed for co-located massive MIMO cellular networks, to cell free networks, jointly with the potential associated constraints. Furthermore, we propose to investigate more particularly the use of widely linear (WL) receivers [50][51], jointly with 1-D constellation, for cell-free MTC networks grant free access based on NB-IoT, potentially combined or not with NOMA schemes.

3 General assumptions and models on low layer

3.1 PHYsical layer

3.1.1 Waveform

The physical layers of 4G and 5G are based on multi-carrier modulation, a.k.a orthogonal frequency-division multiplexing (OFDM). 5G-NR introduced the concept of numerology which consists in increasing the InterCarrier spacing (ICS) to cope with the mobility challenges and take advantage of millimeter wave spectrums [25]. The ICS is defined as $\Delta_f = 15 \times 2^{\mu}$ kHz, where μ is the numerology parameter. This technique maintains compatibility with the 3GPP framework in terms of channel coding, synchronization, channel estimation, physical channel assignment, etc

In the framework of our study, we will be interested in the 5G-NR waveform. It also includes the IoT version (narrow band IoT) as well. The inter-carrier spacing is defined to 3.75 kHz.

3.1.2 Framing

We propose, at the physical layer level, to follow the 5GNR standard for the definition of physical data formats. Figure 20 reminds the format and the semantic used by 3GPPP. A radio frame is composed of 10 subframes, with each subframe divided into 4 slots. A slot is built from 14 OFDM symbols. The unitary resource (carrier/OFDM) is known as resource element (RE). A 12 x 14 array of REs forms a resource block (RB).

Operating in TDD mode, a slot is divided into dedicated UL and DL resources. An example is provided in Figure 20 with 7 symbols dedicated to UL and 7 symbols to DL.For channel estimation purpose, we propose a common RE framing. The demodulation reference signal (DMRS) consists of the pilot symbols that are transmitted in specified REs and used for channel estimation. As shown in Figure 21 and Figure 22, two pilot allocation formats are proposed.

The first format, labelled X**U**Y, is a “structured” format (see Figure 21) able to manage X users (without pilot contamination); Y formats are possible, Y in [0..X-1]. With this format DMRS are orthogonal in time and frequency. Implicitly, we assume that the channel is quasi-constant (in time and frequency) whithin a RB. Nevertheless, it is possible to consider time & frequency interpolation between RBs.

The second format, labelled as RXUY, is a pseudo random format (see Figure 22) able to manage X users. For this format, we proposed to use orthogonal sequence, e.g Zadoff Chu sequence. The channel coefficient associated to the RB is estimated by projecting the received signal into the reference sequence. As X sequences are orthogonal (under the assumption of a constant channel in a RB), it is possible to extract all the channel coefficients from the users (UL channel estimation).

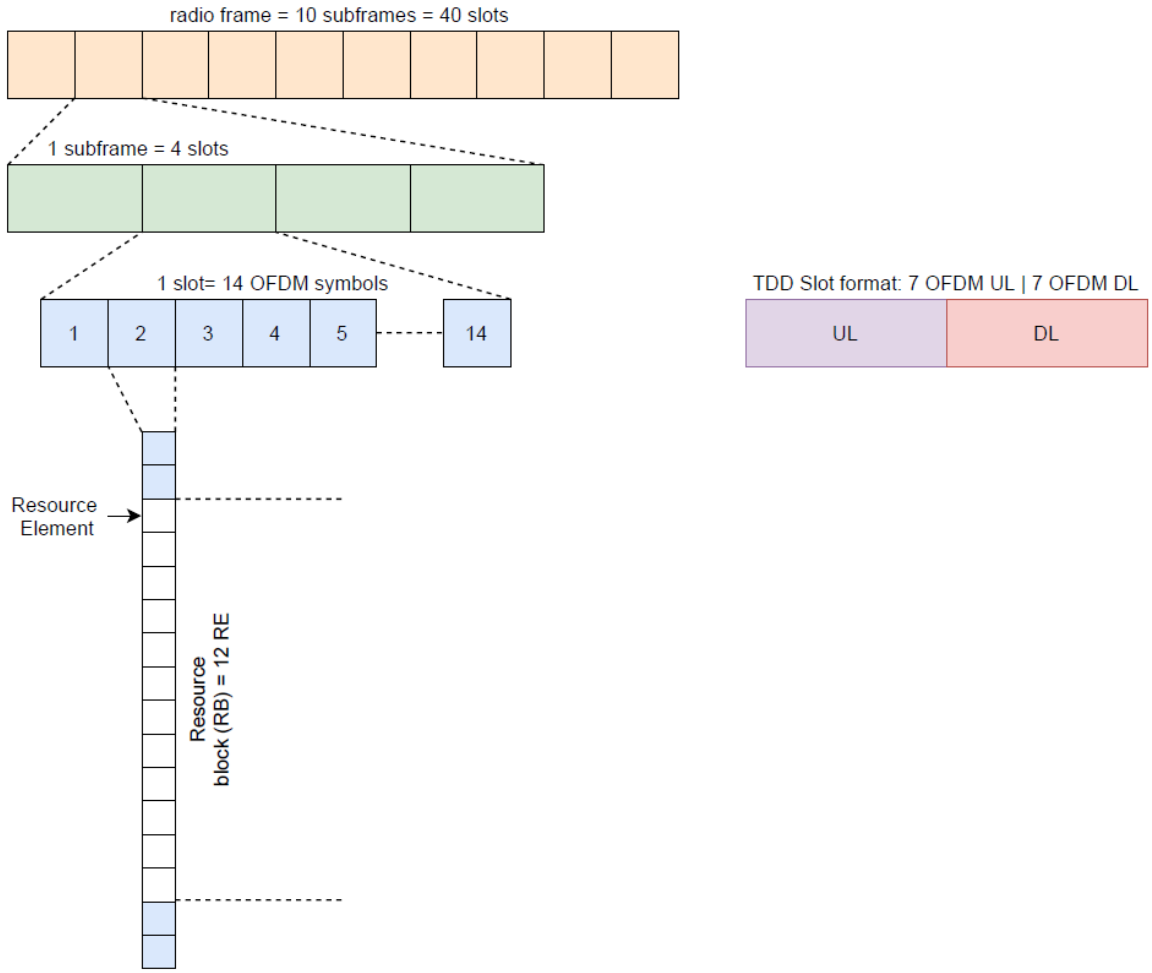

Figure 20 – Framing structure proposed for the studies based on 5GNR format.

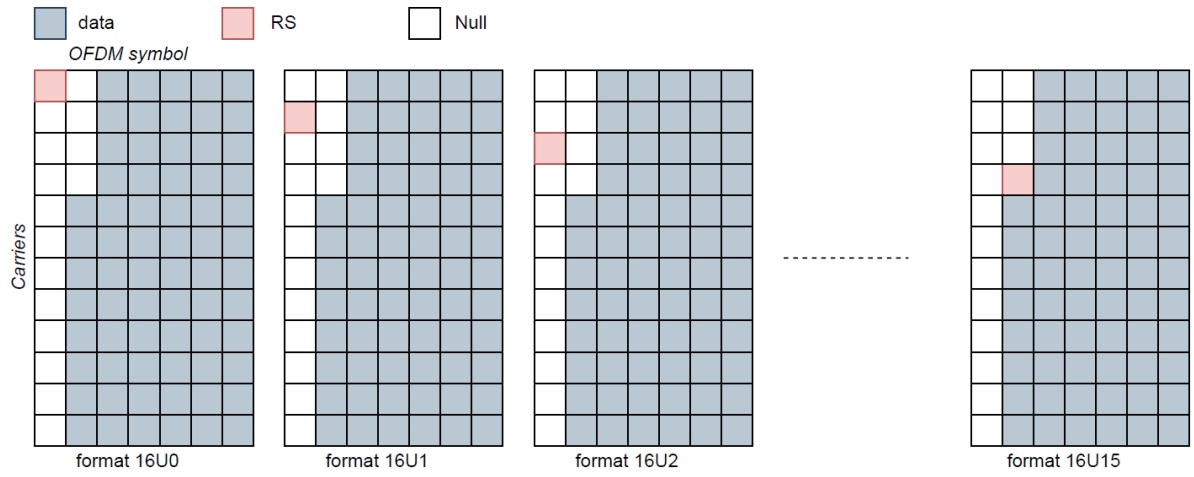

Figure 21 – RB allocation with structured pilot insertion.

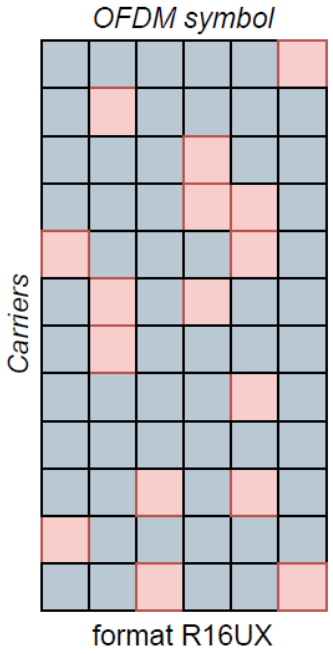

Figure 22 – RB allocation with random pilot insertion.

In case of NB-IoT, the framing strategy is depicted in Figure 23. Here, a slot is composed of 7 OFDM symbols sampled at 3.84MHz. A RB is built with 48 sub-carriers (48 x 3.75kHz = 180 kHz). The slot duration is 2 ms. A blank of 75 µs is inserted every 7 OFDM symbols.

	symb 0		symb 1		symb 2		symb 3		symb 4		symb 5		symb 6		blank	TOTAL
	CP	FFT	CP	FFT	CP	FFT	CP	FFT	CP	FFT	CP	FFT	CP	FFT	blank	
samples	32	1024	32	1024	32	1024	32	1024	32	1024	32	1024	32	1024	288	7680 samples
duration [ms]	0.275		0.275		0.275		0.275		0.275		0.275		0.275		0.075	2 ms

Figure 23 – NB-IoT slot definition.

3.2 Hardware impairments

3.2.1 Power amplifier model

In the case of nonlinear OFDM based CF-mMIMO, the modulated signals are fed, towards each AP antennas, through transmit chains with power amplifiers (PAs). This latter can be characterized by amplitude-to-amplitude (AM/AM) and amplitude-to-phase (AM/PM) conversions. According to the modified Rapp model [26] which has the advantage of exhibiting greater simplicity and accuracy than other models, AM/AM and AM/PM conversions of the solid state power amplifier (SSPA) can be represented as follows:

$$F_{AM-AM}(\rho) = \frac{G\rho}{\left[1 + \left|\frac{G\rho}{V_{sat}}\right|^{2p}\right]^{1/p}}$$

$$F_{AM-PM}(\rho) = \frac{A\rho^q}{\left(1 + \left[\frac{\rho}{B}\right]^q\right)}$$

Where ρ is a modulus of the input signal, G is the PA gain in the linear region, V_{sat} is the PA saturation at the output, p is the smoothness factor that controls the nonlinearity and A, B and q are fitting parameters. The output of the PA can be expressed as :

$$z = F_A(\rho)\, e^{j(\varphi + F_p(\rho))}$$

where φ is the phase of the input signal.

Figure 24 depicts AM/AM and AM/PM conversion characteristics of the modified Rapp PA model for $G = 16, Vsat = 1.9, p = 1.1, A = -345, B = 0.17, q = 4$ as well as the simple clipping PA model. Note that with this later, there is no phase distortion i.e. no AM/PM distortion. With the modified Rapp PA model, which resembles more closely to realistic PAs, both amplitude (AM/AM) and phase (AM/PM) distortions are modelled.

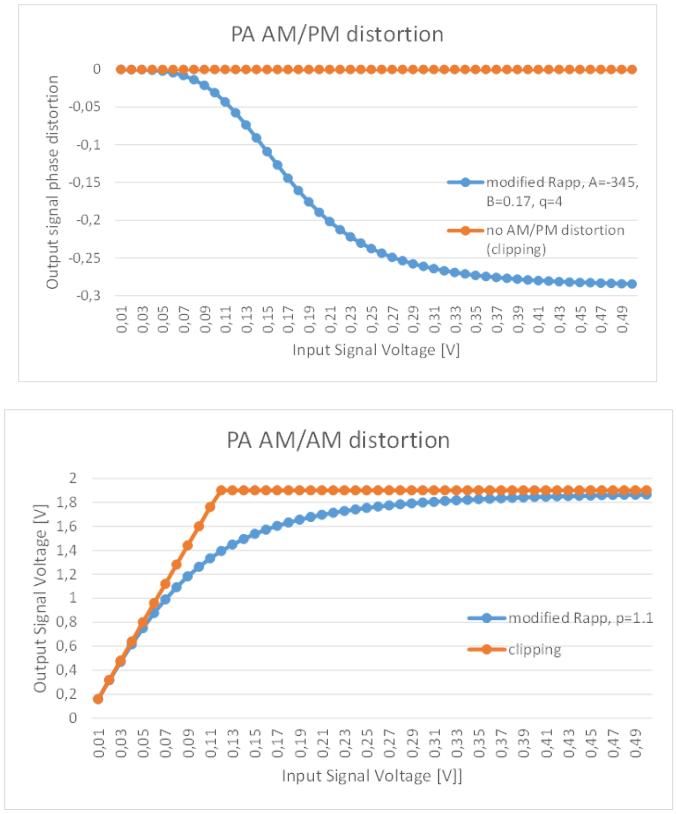

Figure 24 – Power Amplifier AM/AM and AM/PM distortions for clipping (only AM/AM distortion) and modified Rapp model (including both AM/AM and AM/PM distortions) [26]

3.2.2 I/Q imbalance model

Several wireless transceiver architectures are covered in the literature such as super-heterodyne, low intermediate frequency and zero-IF or direct-conversion architectures. Direct-conversion transceivers are regarded as a promising radio architecture in CF-mMIMO [27] since they are expected to make use of low power consumption, low cost and low precision hardware components. In the direct-conversion transceiver architecture, the baseband system is converted directly to the radio-frequency stage and vice versa, hence making it simpler and more cost effective. However, due to the hardware imperfections, there are certain practical challenges involved with this architecture including local oscillator leakages, phase noise, carrier frequency offset, direct current offset, and in-phase and quadrature-phase imbalance. These impairments introduce in-band and out-of-band interference terms and degrade the performance of wireless systems. The in-phase and quadrature-phase (IQ) imbalance occurs due to the mismatch between the real and imaginary parts of the complex signal components and it can cause severe performance degradations especially on OFDM receivers. Moreover, in TDD mMIMO-OFDM system, the (IQ) imbalance tends to destroy the channel reciprocity and degrade the system performance.

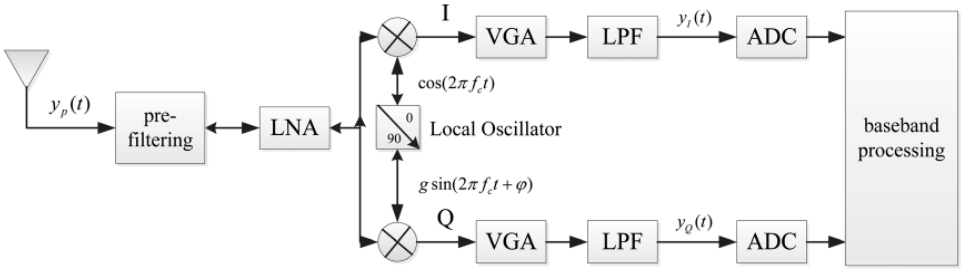

Figure 25 - Direct-conversion or zero-IF transceivers structure [28]

As shown in Figure 25, several stages in the receiver structure can contribute to the IQ imbalance such as the difference of amplitude transfer between in-phase and quadrature-phase branches, as well as, errors in nominal 90° phase shift between the local oscillator signals. The IQ imbalance can be modelled in either a symmetrical or asymmetrical fashion. It can be noted that these two models are mathematically equivalent using a linear transformation [29]. In the POSEIDON project, the asymmetrical IQ imbalance model will be adopted, because it has been extensively used in most relevant works. The baseband equivalent received signal for the n-th antenna element where the IQ imbalance effect appears can be modelled as follows:

$$r_{imb,n} = K_{1,n} \times r_n + K_{2,n} \times r_n^*$$

where the asterisk denotes complex conjugation, r_n is the baseband equivalent signal under ideal IQ matching. The IQ imbalance coefficients $K_{1,n}$ and $K_{2,n}$are given by

$$K_{1,n} \triangleq \left(1 + g_n e^{-j\varphi_n}\right)/2$$

and

$$K_{2,n} \triangleq \left(1 - g_n e^{-j\varphi_n}\right)/2$$

,where $g_n$and φ_n denote the received amplitude and phase mismatch, respectively. We can denote that for perfect IQ matching, the imbalance parameters are g_n*=1* and φ_n*=0*. The ratio between the squared amplitudes of the IQ imbalance coefficients is defined as Image Rejection ratio (IRR) written as:

$$IRR \triangleq \left|K_{1,n}\right|^2 / \left|K_{2,n}\right|^2$$

A similar sort of IQ imbalance might arise at the transmitter side. However, in the POSEIDON project, we assume that the transmitter is self-calibrated which is in line with contemporary system designs. Usually, the I/Q imbalance can be considered constant over the bandwidth of the signal and is therefore independent of the frequency. However, in the case of wideband receivers, the IQ imbalance depends on the frequency (or frequency selective), since the low-pass filters in the I and Q paths are not identical and have different gains, cut-off frequencies, and group delay [30]. Therefore, in wideband receivers, the overall IQ imbalance can be modelled as the sum of frequency dependent

components (due to mixers) and the frequency-dependent IQ component (due to the analog I and Q path filters) as presented in Figure 26.

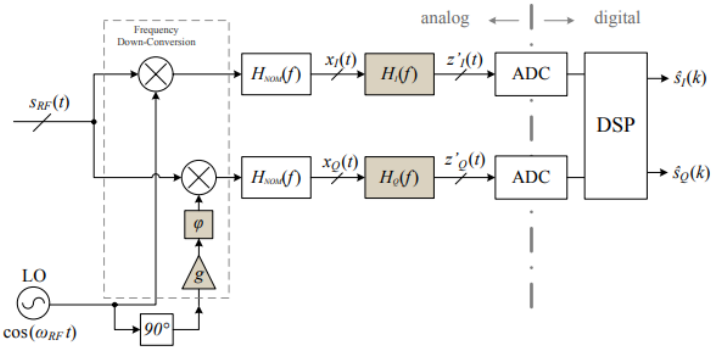

Figure 26 - Overall IQ imbalance front-end model considering dependent and independent frequency IQ components [28]

In Figure 26, $H_{nom}(f)$ is the low-pass filter response which is common for the I and Q branches, HI(f) and HQ(f) are the frequency response distortions of the common low-pass filter.

3.2.3 Quantization noise model

Despite the fruitful research in the literature, most current works on CF-mMIMO assume that perfect analog-to-digital converters (ADCs) and perfect digital-to-analog converters (DACs) were used at access points and user equipments. However, this assumption is impractical for communication networks promoting energy and spectral efficiency. One reason is that the power consumption of ADC increases roughly in an exponential manner with the number of quantization bits and linearly with the sampling rate [31][32]. Hence, the higher the number of antennas at the AP and UE, the higher the power consumption at the AP and UE. Another reason is that the use of low-cost and low-power consumption components is a crucial factor in making CF-mMIMO systems economically viable.

In order to address this challenge efficiently,, the ADC power consumption could be reduced through various methods such as reducing the bit resolution, up-scaling the number of antennas, or keeping the number of users constant [33]. Therefore, uniform low-resolution ADCs and mixed-ADC architecture with a relatively small number of high-resolution ADCs have drawn extensive research interest [34][35][36][37]. In the POSEIDON project, the Bussgang decomposition method will be adopted to model the effect of uniform and non-uniform quantizer. The Bussgang decomposition reformulates the non-linear quantizer model using an equivalent linear model plus quantization noise as shown in Figure 27.

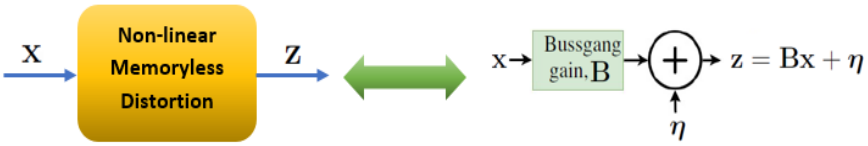

Figure 27 - Generalized Bussgang decomposition for non-linear memoryless distortion [38]

3.2.4 Oscillator phase noise model

Theoretically, APs and UEs use local oscillators (i.e. perfect sinusoidal waves with stable frequency and phase references) to convert baseband signals into passband signals at the transmitter side and to convert passband signals back to the baseband at the receiver side. However, perfect sinusoidal wave generation is unrealistic in practical systems due to thermal, shot and flicker noises in the radio-frequency circuits. Therefore, oscillator phase noise is an inevitable hardware impairment that should be considered in realistic CF-mMIMO systems. In general, phase noise (PN) evolves fast and it is not possible to fully synchronize the APs only by exchanging the fronthaul information. In POSEIDON project, we assume that each AP and each UE has its own free-running local oscillator and at each symbol interval, the phase noise affects the phase of the transmitted symbol. The following discrete-time Wiener phase model will be considered in the nth symbol interval [39][40][41]:

$$\varphi_k[n] = \varphi_k[n-1] + \delta^{\varphi_k}[n], \quad \delta^{\varphi_k}[n] \sim N(0, \sigma^2_{\varphi_k})$$
$$\theta_m[n] = \theta_m[n-1] + \delta^{\theta_m}[n], \quad \delta^{\theta_m}[n] \sim N(0, \sigma^2_{\theta_m})$$

Where $\varphi_k[n]$ and $\theta_m[n]$ denote the phase sample at the kth UE and the mth AP, respectively. $\sigma^2_{\varphi_k}$ and $\sigma^2_{\theta_m}$ denote the phase noise increment variances at the kth UE and the mth AP, respectively. For simplicity's sake, we assume that all oscillators at the APs have the same quality and so do for all UEs (i.e. $\sigma^2_{\theta_m} = \sigma^2_{\theta}, \sigma^2_{\varphi_k} = \sigma^2_{\varphi}, \ \forall\, m, k$). Specifically, $\sigma^2_{\theta} = 4\pi^2 f_c c_\theta T_s$ where f_c is the carrier frequency, T_s is the symbol interval, and c_θ is a constant dependent on the oscillator. Similarly, $\sigma^2_{\varphi} = 4\pi^2 f_c c_\varphi T_s$.

3.3 Calibration model

The objective of this section is to give a standard model for calibrating of algorithms based on a probabilistic modelling of the propagation channel to facilitate the tuning and the comparison with the state of the art. The project will go further than these models by integrating a numerical twin of the propagation.

We let the frequency-domain channel coefficient $h_{l,k,n} \in C^{M\times 1}$ between the l-th AP and the k-th UE at subcarrier n, where M is the number of antennas per AP, $n = 0, \ldots, N-1$ and N denotes the total number of OFDM subcarriers.

A block-fading channel is considered, which is constant during a time-frequency interval, known as the coherence interval, and varies independently between coherence intervals. Besides, we assume that the large-scale fading coefficients vary slowly, i.e., they are constant over many coherence intervals.

Then, they are assumed to be known at each AP and they are used afterwards to estimate the frequency-domain channel responses.

$h_{l,k,n}$ can be modeled as independent and identically distributed (i.i.d.) circularly symmetric Gaussian entries $h_{l,k,n} \sim CN(0, I_M \beta_{l,k})$, where $\beta_{l,k}$ denotes the large-scale fading which is frequency and antenna independent and can be written as [6]

$$\beta_{l,k} = PL_{l,k}.10^{\frac{\sigma_{sh} z_{l,k}}{10}}$$

where $PL_{l,k}$ denotes the path-loss and $10^{\frac{\sigma_{sh} z_{l,k}}{10}}$ models the log-normal shadow fading with standard deviation σ_{sh} and $z_{l,k} \sim N(0,1)$. We consider the 3GPP Urban Microcell path-loss model [42, Table B.1.2.1-1]], which is written as

$$PL_{l,k}[dB] = -22.7 - 36.7 log_{10}\left(\frac{d_{l,k}}{1\ m}\right) - 26 log_{10}\left(\frac{f_c}{1\ GHz}\right)$$

where f_c is the carrier frequency and $d_{l,k}$ denotes the distance between the l-th AP and the k-th UE including AP and UE's heights.

4 Conclusions

Document D1.1 sets the stage for the technical and demonstration activities carried out as part of the POSEIDON project, specifying the frequency bands to be considered, the target requirements, the relevant performance indicators and the B5G scenarios.

Few scenarios are being studied and initial results illustrated. In particular, the use of new bands around 6 and 7 GHz seems interesting for eMBB use case. In fact, despite the propagation loss inherent in higher frequencies (albeit limited), these frequencies make it possible to address a new spectrum, and for the same number of antennas, the footprint is reduced. Detailed modelling of the propagation channel should enable us to benchmark a cell-free MIMO solution with a mMiMO solution as we know it today for 5G in the 3.5GHz bands. The digital twin tool should also enable the benefits of the proposed solutions to be quantified (throughput, end-to-end energy efficiency...).

The scenario of dense private networks is also considered important. At the scale of a small deployment, a cell-free MIMO solution appears to meet many of the eMMB and URLLC KPIs. Indeed, the use of macro-diversity can clearly improve quality of service; however, challenges remain, particularly in terms of clustering, dynamic allocations (clustering, power) and initial access. In addition, we have undertaken to evaluate grant-free access in a CF-mMIMO network. These studies will initially be based on a stochastic channel.

The next deliverable, D1.2. “Channel models, samples and network deployment strategies” will provide relevant channel models, channel samples as well as per-use-case network deployment.

Bibliography

[1] T. L. Marzetta, “Noncooperative cellular wireless with unlimited numbers of base station antennas,” IEEE Trans. Wireless Commun., vol. 9, no. 11, pp. 3590-3600, Nov. 2010.

[2] N. Rajatheva and e. al., “White paper on broadband connectivity in 6G,” 2020.

[3] Ö Bulakçı, Xi Li, M Gramaglia, A Gavras, M Uusitalo, P Rugeland , Mauro Boldi, "Towards Sustainable and Trustworthy 6G: Challenges, Enablers, and Architectural Design", June 2023. Boston-Delft: now publishers, http://dx.doi.org/10.1561/9781638282396

[4] E. Bjornson and L. Sanguinetti, “Scalable cell-free massive MIMO systems,” IEEE Trans. Commun., vol. 68, no. 7, pp. 4247-4261, Jul. 2020.

[5] G. Interdonato, M. Karlsson, E. Bjornson, and E. G. Larsson, “Local Partial Zero-Forcing Precoding for Cell-Free Massive MIMO,” IEEE Transactions on Wireless Communications, vol. 19, no. 7, pp. 4758–4774, 2020.

[6] J. Zhang, J. Zhang, E. Bj¨ornson, and B. Ai, “Local Partial Zero-Forcing Combining for Cell-Free Massive MIMO Systems,”, IEEE Transactions on Communications, vol. 69, no. 12, pp. 8459–8473, 2021

[7] Ericsson, “Ericsson Mobility Report”, November 2022.

[8] S. Suardi and P. Castells, "The Socio-Economic Benefits of Mid-Band 5G Services," February 2022.

[9] M. Norin, R. Högman, M. Buchmayer, G. Lemme, F. Pedersen and A. Zaidi, “White Paper - 5G Spectrum for local industrial networks,” April 2022.

[10] Wi-Fi Alliance, “6 GHz Wi-Fi: Connecting to the future”, October 2022.

[11] GSMA Association, “The 6 GHz IMT Ecosystem Demand Drives Scale”, August 2022.

[12] ITU, Recommendation ITU-R P.2109-1, « Prediction of building entry loss », Aug. 2019.

[13] "3GPP TR 38.801 v14.0.0", *3rd Generation Partnership Project; Technical Specification Group Radio Access Network; Study on new radio access technology: Radio access architecture and interfaces (Release 14)*, Apr. 2017.

[14] L. Furtado, A. Fernandes, A. Ohashi, F. Farias, A. Cavalcante and J. Costa, "Cell-Free Massive MIMO Deployments: Fronthaul Topology Options and Techno-Economic Aspects," *2022 16th European Conference on Antennas and Propagation (EuCAP)*, Madrid, Spain, 2022.

[15] Özlem Tuğfe Demir, Meysam Masoudi, Emil Björnson, Cicek Cavdar, “Cell-Free Massive MIMO in O-RAN: Energy-Aware Joint Orchestration of Cloud, Fronthaul, and Radio Resources”, Signal Processing (eess.SP); Information Theory (cs.IT), arXiv:2301.06166. Janv 2023.

[16] V. Ranjbar, A. Girycki, M. A. Rahman, S. Pollin, M. Moonen and E. Vinogradov, "Cell-Free mMIMO Support in the O-RAN Architecture: A PHY Layer Perspective for 5G and Beyond Networks," in *IEEE*

Communications Standards Magazine, vol. 6, no. 1, pp. 28-34, March 2022, doi: 10.1109/MCOMSTD.0001.2100067.

[17] ETSI, TR 128.901 v16.1.0, “5G; Study on channel model for frequencies from 0.5 to 100 GHz”.

[18] WRC-23 : 5G For All, Harmonisation, capacity and cost, The GSMA WRC Series

[19] UK telecoms regulator Ofcom, Evolution of the Shared Access Licence Framework, 28 March 2023, https://www.ofcom.org.uk/__data/assets/pdf_file/0032/255965/call-for-inputs-evolution-of-shared-access.pdf

[20] SHEN, Xuemin, GAO, Jie, LI, Mushu, et al. Toward Immersive Communications in 6G. arXiv preprint arXiv:2303.05283, 2023.

[21] http://www.mosaic-lab.org/uploads/papers/d9cf64f9-9f50-4f15-b2d1-886b3c9e08ff.pdf

[22] 5G Services Innovation – 5G Americas White Paper, https://www.5gamericas.org/wp-content/uploads/2019/11/5G-Services-Innovation-FINAL-1.pdf

[23] 5G European Validation platform for Extensive trials (5G EVE), Deliverable D1.2, Requirements definition and analysis from vertical industries and core applications, 2019, https://www.5g-eve.eu/wp-content/uploads/2019/11/5g-eve-d1.2-requirements-definition-analysis-vertical-industries-core-applications.pdf

[24] ETSI, TS 122.261 v15.9.0 (2021-10), “5G; Service requirements for the 5G system” (3GPP TS 22.261 version Release 15).

[25] 3GPP, “NR: Physical channels and modulation,” Tech. Spec. Group Radio Access Netw. Rel. 17 TS 38.211 v. 17.1.0, 2022-April.

[26] Nokia, “Realistic Power Amplifier Model for the New Radio Evaluation,” document R4-163314, 3GPP TSG-RAN WG4 Meeting 79, 2016.

[27] A. Papazafeiropoulos, E. Björnson, P. Kourtessis, S. Chatzinotas and J. M. Senior, "Scalable Cell-Free Massive MIMO Systems: Impact of Hardware Impairments," in *IEEE Transactions on Vehicular Technology*, vol. 70, no. 10, pp. 9701-9715, Oct. 2021.

[28] S. Zhang, Y. Tian, P. Ye, L. Guo, H. Zeng and H. Li, "A Novel Calibration Method of DC-Offsets in Direct-Conversion Transmitter," in *IEEE Comm Letters*, vol. 26, no. 11, pp. 2745-2749, Nov. 2022.

[29] N. Kolomvakis, M. Matthaiou, and M. Coldrey, “IQ imbalance in multiuser systems: Channel estimation and compensation,” IEEE Trans. Comm.., vol. 64, no. 7, pp. 3039–3051, Jul. 2016.

[30] M. Valkama, M. Renfors and V. Koivunen, "Compensation of frequency-selective I/Q imbalances in wideband receivers: models and algorithms," *2001 IEEE Third Workshop on Signal Processing Advances in Wireless Communications (SPAWC'01). Workshop Proceedings*, pp. 42-45, Taiwan, 2001.

[31] Y. Zhang, M. Zhou, H. Cao, L. Yang and H. Zhu, "On the Performance of Cell-Free Massive MIMO With Mixed-ADC Under Rician Fading Channels," in *IEEE Communications Letters*, vol. 24, no. 1, pp. 43-47, Jan. 2020

[32] Y. Zhang, M. Zhou, X. Qiao, H. Cao and L. Yang, "On the Performance of Cell-Free Massive MIMO With Low-Resolution ADCs," in *IEEE Access*, vol. 7, pp. 117968-117977, 2019,

[33] M. Sarajlić, L. Liu and O. Edfors, "When Are Low Resolution ADCs Energy Efficient in Massive MIMO?," in *IEEE Access*, vol. 5, pp. 14837-14853, 2017

[34] Y. Zhang, M. Zhou, X. Qiao, H. Cao and L. Yang, "On the Performance of Cell-Free Massive MIMO With Low-Resolution ADCs," in *IEEE Access*, vol. 7, pp. 117968-117977, 2019

[35] Y. Xiong, S. Sun, N. Wei, L. Liu and Z. Zhang, "Asymptotic Analysis for Cell-Free Massive MIMO With MMSE Combining and Low-Resolution ADCs," in *IEEE Communications Letters*, vol. 25, no. 10, pp. 3219-3223, Oct. 2021

[36] Y. Zhang, M. Zhou, H. Cao, L. Yang and H. Zhu, "On the Performance of Cell-Free Massive MIMO With Mixed-ADC Under Rician Fading Channels," in *IEEE Communications Letters*, vol. 24, no. 1, pp. 43-47, Jan. 2020

[37] Y. Zhang, Y. Cheng, M. Zhou, L. Yang and H. Zhu, "Analysis of Uplink Cell-Free Massive MIMO System With Mixed-ADC/DAC Receiver," in *IEEE Systems Journal*, vol. 15, no. 4, pp. 5162-5173, Dec. 2021.

[38] O. T. Demir and E. Bjornson, "The Bussgang Decomposition of Nonlinear Systems: Basic Theory and MIMO Extensions [Lecture Notes]," in *IEEE Signal Processing Magazine*, vol. 38, no. 1, pp. 131-136, Jan. 2021.

[39] H. Ghozlan and G. Kramer, "Models and Information Rates for Wiener Phase Noise Channels," in *IEEE Transactions on Information Theory*, vol. 63, no. 4, pp. 2376-2393, April 2017

[40] Y. Fang, L. Qiu, X. Liang and C. Ren, "Cell-Free Massive MIMO Systems With Oscillator Phase Noise: Performance Analysis and Power Control," in *IEEE Transactions on Vehicular Technology*, vol. 70, no. 10, pp. 10048-10064, Oct. 2021

[41] Y. Fang, X. Li and L. Qiu, "Asymptotic equivalent performance of uplink massive MIMO systems with phase noise", *Proc. IEEE Int. Conf. Commun.*, pp. 1-6, 201

[42] 3GPP, “Further advancements for E-UTRA physical layer aspects (release 9),” 3GPP TS 36.814, 3rd Generation, Partnership Project (3GPP), Mar. 2017.

[43] C. Bockelmann, N. Patras, H. Nikopour, K. Au, T. Svensson, C. Stefanovic, P. Popovski, A. Dekorsy, "Massive Machine-Type Communications in 5G: Physical and MAC-Mayer Solutions", *IEEE Communications Magazine, pp. 59-65, Sept. 2016*

[44] J. Xu, J. Yao, L. Wang, Z. Ming, K. Wu, L. Chen, "Narrowband Internet of Things: Evolutions, Technologies, and Open Issues", *IEEE Internet of Things Journal, Vol.5, N°3, pp. 1449-1462, June 2018*

[45] G. Berardinelli et al., "Reliability analysis of uplink grant-free transmission over shared resources", *IEEE Access, Vol.6, pp. 23602-23611, 2018*

[46] Z. Ding, X. Lei, G.K. Karagiannidis, R. Shoeber, J. Yuan, V.K. Bhargava,"A survey on non-orthogonal multiple access for 5G networks: Research challenges and future trends", *IEEE J. Sel. Areas Commun, Vol.35, N°10, pp. 2181-2195, Oct. 2017*

[47] L. Liu, W. Yu,"Massive connectivity with massive MIMO – Part I: Device activity detection and channel estimation", *IEEE Trans. Signal Processing, Vol.66, N°11, pp. 2933-2946, June 2018*

[48] A. Bayesteh, E. Yi, H. Nikopour, H. Baligh,"Blind detection of SCMA for uplink grant free multiple-access", *Proc. Int. Symposium Wireless Communi. Systems (ISWCS), Vol.66, N°11, pp. 853-857, 2014*

[49] M. Mohammadkarimi, M.A. Raza, O.A. Dobre,"Signature-based non-orthogonal massive multiple access for future wireless networks: uplink massive connectivity for machine type communications", *IEEE Vehicular Technology Magazine, Vol.13, N°4, pp. 40-50, Oct. 2018*

[50] B. Picinbono, P. Chevalier,"Widely linear estimation with complex data", *IEEE Trans. Signal Processing, Vol.43, N°8, pp. 2030-2033, Aug. 1995*

[51] P. Chevalier, F. Pipon, "New Insights into optimal Widely Linear array receivers for the demodulation of BPSK, MSK and GMSK signals corrupted by noncircular interferences – Application to SAIC", *IEEE Trans. Signal Processing, Vol.54, N°3, pp. 870-883, March 2006*

[52] R. Gui, N.M. Balasubramanya, L. Lampe, "Connectivity Performance Evaluation for Grant-Free Narrowband IOT with Widely Linear Receivers", *IEEE Internet of Things Journal, Vol.7, N°10, pp. 10562-10572, Oct. 2020.*